Article

Cell Reports

Maf1 and Repression of RNA Polymerase III-Mediated Transcription Drive Adipocyte Differentiation

Graphical Abstract

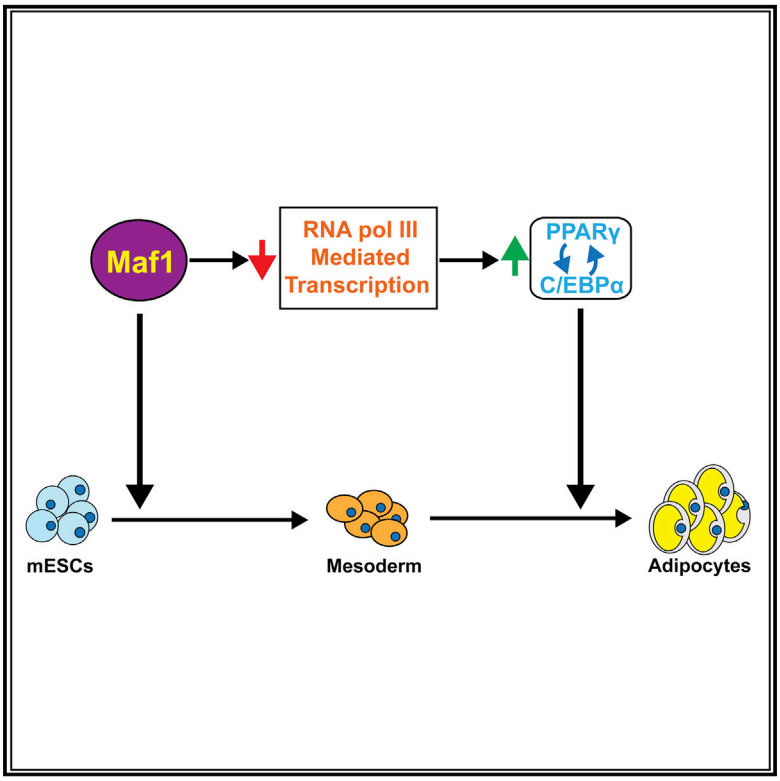

Authors

Chun-Yuan Chen, Rainer B. Lanz, Christopher J. Walkey, Wen-Hsuan Chang, Wange Lu, Deborah L. Johnson

Correspondence

deborah.johnson@bcm.edu

In Brief

Maf1 and RNA pol III transcription repression play a key role in cell fate determination by promoting mesoderm induction and adipocyte differentiation. Chen et al. show that alterations in RNA pol III transcription produce select changes in adipogenic genes, and inhibitory factors including Wnt6 and H19lnc RNA, to regulate adipogenesis.

Highlights

- The transcriptional repressor Maf1 promotes mesoderm induction of mESCs
- Maf1 represses RNA pol III-mediated transcription to induce adipogenesis
- Altered RNA pol III activity produce gene signatures for adipocyte differentiation
- RNA pol III repression reduces Wnt6 and H19lnc RNA expression to enhance adipogenesis

Data and Software Availability

GSE113324

Chen et al., 2018, Cell Reports *24*, 1852–1864
August 14, 2018
https://doi.org/10.1016/j.celrep.2018.07.046

CellPress

OPEN ACCESS
CellPress

Cell Reports
Article

Maf1 and Repression of RNA Polymerase III-Mediated Transcription Drive Adipocyte Differentiation

Chun-Yuan Chen,[1,2] Rainer B. Lanz,[2] Christopher J. Walkey,[2] Wen-Hsuan Chang,[3] Wange Lu,[1,3] and Deborah L. Johnson[2,4,*]

[1]Department of Biochemistry and Molecular Biology, University of Southern California, Los Angeles, CA, USA
[2]Department of Molecular and Cellular Biology and the Dan L. Duncan Cancer Center, Baylor College of Medicine, Houston, TX, USA
[3]Eli and Edythe Broad Center for Regenerative Medicine and Stem Cell Research, University of Southern California, Los Angeles, CA, USA
[4]Lead Contact
*Correspondence: deborah.johnson@bcm.edu
https://doi.org/10.1016/j.celrep.2018.07.046

SUMMARY

RNA polymerase (pol) III transcribes a variety of small untranslated RNAs involved in transcription, RNA processing, and translation. RNA pol III and its components are altered in various human developmental disorders, yet their roles in cell fate determination and development are poorly understood. Here we demonstrate that Maf1, a transcriptional repressor, promotes induction of mouse embryonic stem cells (mESCs) into mesoderm. Reduced Maf1 expression in mESCs and preadipocytes impairs adipogenesis, while ectopic Maf1 expression in *Maf1*-deficient cells enhances differentiation. RNA pol III repression by chemical inhibition or knockdown of Brf1 promotes adipogenesis. Altered RNA pol III-dependent transcription produces select changes in mRNAs with a significant enrichment of adipogenic gene signatures. Furthermore, RNA pol III-mediated transcription positively regulates long non-coding RNA H19 and Wnt6 expression, established adipogenesis inhibitors. Together, these studies reveal an important and unexpected function for RNA pol III-mediated transcription and Maf1 in mesoderm induction and adipocyte differentiation.

INTRODUCTION

RNA polymerase (pol) III transcribes genes that encode a variety of small untranslated RNAs, including tRNAs, 5S rRNAs, and U6 RNAs (Turowski and Tollervey, 2016). RNA pol III products play important roles in protein synthesis, protein trafficking, transcription elongation, and RNA processing. The rate of transcription is tightly regulated to correspond to the metabolic and proliferative demands of cells. Maf1, initially identified in yeast (Boguta et al., 1997; Upadhya et al., 2002), associates with RNA pol III to inhibit transcription (Desai et al., 2005). In addition to Maf1-mediated repression of RNA pol III-dependent genes, mammalian Maf1 is recruited to select RNA pol II-dependent gene promoters to repress (Johnson et al., 2007; Lee et al., 2015; Li et al., 2016; Palian et al., 2014) or activate (Li et al., 2016) transcription. Maf1 negatively regulates lipogenic enzyme gene expression and intracellular lipid accumulation both *in vitro* and *in vivo* (Khanna et al., 2014; Palian et al., 2014). This function is conserved as Maf1 controls lipid homeostasis in *C. elegans* (Khanna et al., 2014). Given that deregulation of Maf1-targeted genes such as tRNAs and 5S rRNAs (Johnson and Johnson, 2008) and lipogenic genes (Baenke et al., 2013) are hallmarks of transformed cells and human cancers, this implicated a potential tumor suppressor role for Maf1. Accordingly, studies revealed that Maf1 inhibits cellular transformation and tumorigenesis and its expression is diminished in human liver cancer (Li et al., 2016; Palian et al., 2014). Enhanced RNA pol III-dependent transcription is necessary to drive oncogenesis (Johnson et al., 2008), and emerging evidence supports the idea that alterations in the expression of specific tRNAs can drive cell proliferation, tumor growth, and metastasis (Clarke et al., 2016; Gingold et al., 2014; Goodarzi et al., 2016). In addition, recent studies implicate a role for RNA pol III-mediated transcription in longevity (Filer et al., 2017).

In contrast to what is known about the function of Maf1 in repressing oncogenesis, little is known about its potential role in other biological processes. Emerging studies are revealing that mutations in RNA pol III and its transcription components are associated with various human disorders (Borck et al., 2015; Daoud et al., 2013; Dauwerse et al., 2011; Girotto et al., 2013; Jee et al., 2017; Thiffault et al., 2015), yet how this transcription process or Maf1 might regulate developmental programs and cell fate determination is not yet known. We therefore examined a potential role for Maf1 in early development and cellular differentiation by using embryonic stem cells (ESCs). These cells have the capacity for prolonged self-renewal, and they are able to differentiate into a variety of specialized cell types (Rippon and Bishop, 2004; Zhao and Jin, 2017). We find that Maf1 protein expression is substantially reduced as both human ESCs (hESCs) and mouse ESCs (mESCs) differentiate into embryoid bodies (EBs) containing the three germ layers, coinciding with enhanced RNA pol III transcript expression. However, although Maf1 does not regulate ESC self-renewal, cellular Maf1 concentrations affect the ability of these cells to form the mesoderm germ layer. Upon further examination of the terminal

differentiation of these cells into adipocytes, we find that Maf1 enhances the expression of the central regulators of adipogenesis, PPARγ and C/EBPα (Rosen et al., 2002; Rosen and MacDougald, 2006), to facilitate this process in mESCs, 3T3-L1 preadipocytes, and mouse embryo fibroblasts (MEFs). Importantly, we find that Maf1-mediated repression of RNA pol III-dependent gene expression contributes to its ability to induce adipogenesis. Adipogenesis was enhanced by chemical inhibition of RNA pol III as well as by downregulation of the RNA pol III-specific transcription factor Brf1. RNA sequencing (RNA-seq) analysis of cells undergoing adipogenesis revealed that altered RNA pol III-dependent transcription produced select changes in gene expression. Maf1 downregulation altered transcripts that were concurrently upregulated by Brf1 knockdown and inhibitor treatment. These changes enriched for a gene expression signature encompassing adipocyte and lipid metabolism. RNA pol III-mediated transcription repression decreased expression of long non-coding (lnc) H19 RNA and Wnt6, consistent with their previously identified roles in negatively regulating adipogenesis. These results identify an unexpected role for RNA pol III-mediated transcription in controlling adipocyte differentiation through its modulation of specific RNA pol II-transcribed genes.

RESULTS

Maf1 Promotes the Induction of mESCs into Mesoderm

Maf1 expression was analyzed in human and mESCs and after they were programmed to differentiate into EBs. Maf1 protein expression was relatively high in both hESCs and mESCs but substantially decreased as the cells differentiated into EBs (Figures 1A and 1C). This occurred without a discernible change in Maf1 mRNA (Figures 1B and 1D) suggesting that Maf1 is regulated post-transcriptionally during this process. Consistent with the decrease in Maf1 protein during differentiation, corresponding increases in the Maf1-targeted RNA pol III-dependent transcripts pre-tRNA^{Leu} and U6 RNA were observed as the ESCs differentiated into EBs. To determine whether Maf1 is required for mESC self-renewal, we reduced its expression using lentiviral delivery of two different short hairpin RNAs (shRNAs) (Figure 1E). Maf1 knockdown in these cells resulted in an increase in U6 RNA (Figure 1F), indicating that Maf1 is functioning to repress transcription in these cells. However, cell accumulation rates were unaffected upon decreased Maf1 expression (Figure 1I). Examination of markers for self-renewal by immunostaining of SSEA1, histochemical staining of alkaline phosphatase, and RT-qPCR analysis of mRNAs for Sox2, Nanog, and Oct4 revealed that there were no significant changes in these markers when Maf1 expression was decreased (Figures 1G and 1H). Thus, altered Maf1 expression does not affect mESC self-renewal or the proliferative capacity of mESCs.

We next assessed whether Maf1 was involved in maintaining mESC pluripotency and the ability of these cells to differentiate into EBs that constitute the three primary germ layers. Examining the expression of markers that specify endoderm (Gata6 and Gata4), mesoderm (T and Mesp1), and ectoderm (Nestin and Sox1) revealed that decreased Maf1 expression in mESCs had a relatively modest effect on the expression of endoderm and ectoderm markers, but a significant decrease was observed in mesoderm marker expression (Figure 2A). Consistent with these results, expression of an HA-tagged Maf1 construct resulted in enhanced expression of both T mRNA and protein (Figures 2B and 2C). These results indicate that Maf1 facilitates cell fate commitment of mouse EBs (mEBs) to into the mesoderm germ layer.

Maf1 Promotes the Differentiation of mESCs into Terminally Differentiated Adipocytes

As Maf1 is involved in regulating lipid homeostasis (Khanna et al., 2014; Palian et al., 2014), and adipocytes are a derivative of the mesoderm lineage, we examined whether Maf1 knockdown in mESCs and the impairment of mesoderm induction might further affect the terminal differentiation of these cells into adipocytes. Decreased Maf1 expression by two different shRNAs in the mESCs resulted in an increase in RNA pol III-generated transcripts (Figure 3A). These cells were then programmed to undergo terminal adipocyte differentiation (Figure S1A). At day 22, pre-tRNA^{Leu} and U6 RNA transcripts were significantly reduced, even in cells that were expressing the Maf1 shRNAs. However, reduced Maf1 expression resulted in a significant decrease in the number of adipocyte colonies (Figure 3C). This was not due to a change in cell number or viability, as the control and Maf1-knockdown cells showed no detectable difference. The change in adipocyte colonies corresponded to a reduction in the expression of two key adipogenic inducers, PPARγ and C/EBPα, and their downstream targets FABP4 and perilipin (Figures 3B and 3C). These results support the idea that Maf1 promotes mESCs to terminally differentiate into adipocytes.

Maf1 Induces Pro-adipogenic Gene Expression and Enhances Adipocyte Differentiation

The observed impairment in adipogenesis by decreased Maf1 expression could be a result of changes in mesoderm induction, which then leads to altered adipogenesis, or Maf1 may additionally play a role in the terminal differentiation of preadipocytes. To address this, we differentiated 3T3-L1 preadipocyte cells into adipocytes (Figure S1B). Maf1 protein expression was increased during the differentiation process (Figures 4B and S2B). However, a reproducible increase in tRNA gene transcripts was also observed (Figures 4A and S2A), suggesting that other factors are determining the overall rate of tRNA synthesis as the 3T3-L1 cells differentiate into adipocytes. Knockdown of Maf1 expression by two different shRNAs in the preadipocytes resulted in an initial slight increase in tRNA gene transcripts that was also marginally increased upon differentiation (Figures 4A and S2A). However, decreased Maf1 expression significantly limited the induction of adipogenic gene mRNAs and proteins (Figures 4A, 4B, S2A, and S2B). Maf1 knockdown further resulted in a corresponding decrease in adipocyte differentiation (Figures 4C and S2C). These results indicate that Maf1 not only functions to enhance the induction of ESCs to form mesoderm but independently drives the terminal differentiation of preadipocytes.

To further confirm a role for Maf1 in adipogenesis, we differentiated *Maf1*$^{-/-}$ MEFs into adipocytes (Figure S1C). Few small adipocyte colonies were observed when the *Maf1*$^{-/-}$ MEFs were programed to differentiate into adipocytes (Figure 5C). Ectopic expression of Maf1 in these cells resulted in a significant

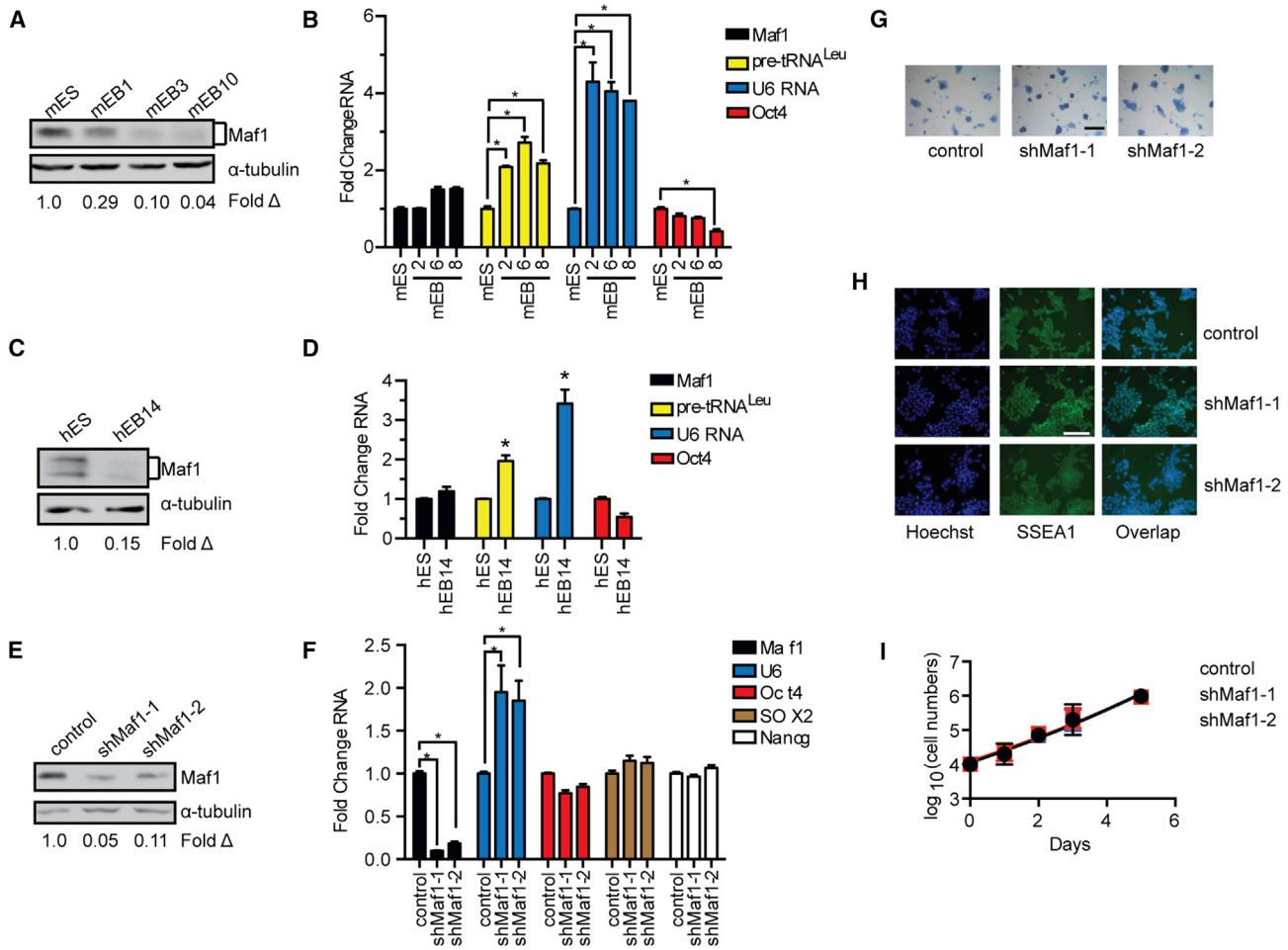

Figure 1. Maf1 Does Not Affect mESC Self-Renewal

(A) Maf1 protein expression in mESCs and mEBs. mEB1, mEB3, and mEB10 represent the number of days after mEB formation. Protein amounts for the immunoblots were normalized to α-tubulin; fold change was calculated relative to Maf1 protein amounts in mESCs.

(B) qRT-PCR of Maf1 and Oct4 mRNA and Maf1 target genes, $tRNA^{Leu}$ and U6 RNA, in mESCs and mEBs at the indicated days. The amount of transcript was normalized to β-actin. The fold change was calculated relative to the amount of transcripts expressed in mESCs.

(C) Maf1 expression in hESCs and hEBs at day 14 (hEB14). Protein amounts for the immunoblots were normalized to α-tubulin, and the fold change was calculated relative to the amount of protein in hESCs.

(D) qRT-PCR analysis of Maf1 and Oct4 mRNA, $tRNA^{Leu}$, and U6 RNA at day 14. The amount of transcript was normalized to β-actin. The fold change was calculated relative to the amount of each transcript in hESCs.

(E) Immunoblot analysis for Maf1 expression that was decreased in mESCs. Immunoblot analysis of Maf1 protein in control and Maf1 knockdown mESCs normalized to α-tubulin. The fold change in Maf1 expression was calculated relative to protein in control mESCs.

(F) qRT-PCR analysis of Maf1, U6 RNA, and self-renewal markers, Oct4, SOX2, and Nanog mRNAs in mESCs. The amount of transcript was normalized to β-actin. The fold change was calculated relative to lentivirus-infected control cells.

(G) Alkaline phosphatase staining of control and Maf1-knockdown mESCs. Scale bar denotes 200 μm.

(H) Immunostaining images of control and Maf1-knockdown mESCs antibody against SSEA1. Scale bar denotes 100 μm.

(I) Cell accumulation rates of control and Maf1-knockdown mESCs. Control and Maf1-knockdown mESCs were plated evenly on day 0, and the cell numbers were counted at the indicated days.

For (B), (D), (F), and (I), data are mean ± SD of n = 3 independent experiments. *p < 0.05, unpaired Student's t test.

decrease in tRNA transcripts throughout the differentiation process. Furthermore, an increase in the expression of the pro-adipogenic gene mRNAs and protein was observed, correlating with an increase in adipocyte formation (Figures 5A–5C). Induction of Maf1 expression for only the first 3 days was sufficient to drive this increase in adipogenesis (Figures S3A and S3B), suggesting that Maf1 acts early in this process to facilitate adipocyte formation. We further determined how a reduction in Maf1 expression in 3T3-L1 cells would affect their ability to form fat tissue *in vivo*. 3T3-L1 cells expressing either control shRNA or Maf1 shRNA were injected into the sternum of athymic mice. Among four mice injected with cells expressing the control shRNA, three developed visible fat pads in the region of the injection. In contrast, none of the mice expressing the shRNA-targeting

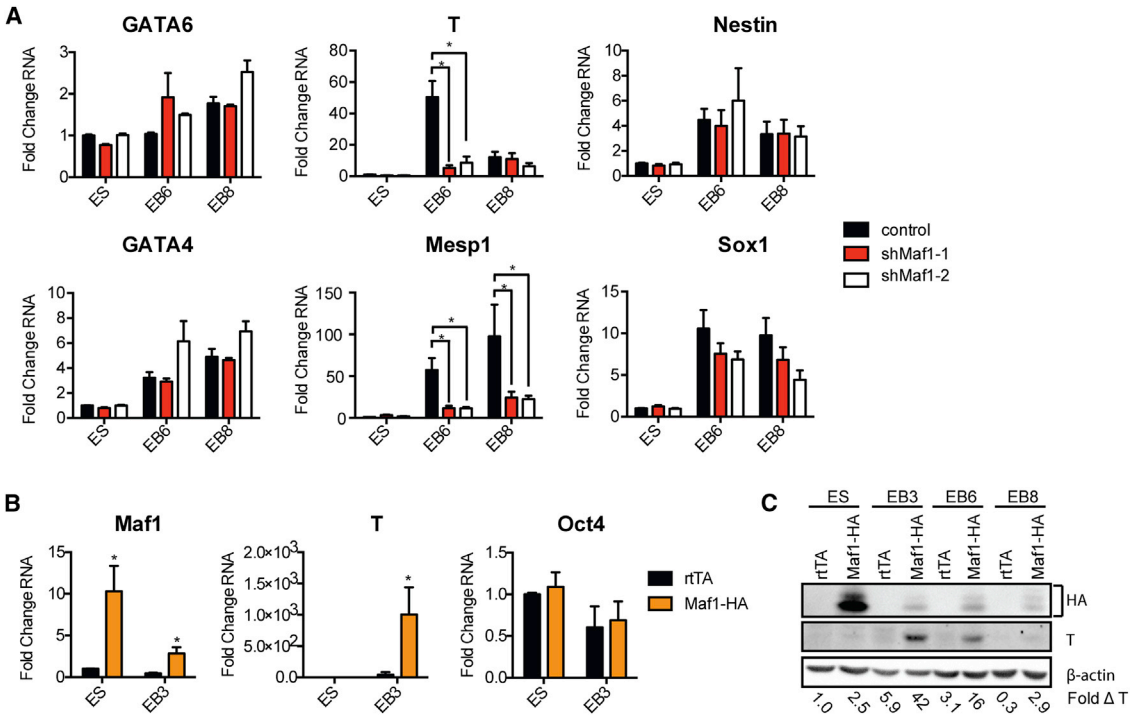

Figure 2. Maf1 Promotes the Expression of Mesodermal Markers in mEBs

(A) qRT-PCR analysis of markers associated with the three germ layers (endoderm: GATA6 and GATA4; mesoderm: T and Mesp1; ectoderm: Nestin and SOX1) in control and Maf1-knockdown mESCs and mEBs at the indicated days after cells were infected with either a control lentiviral construct or one harboring an shRNA-targeting Maf1 mRNA.

(B) qRT-PCR analysis of Maf1, T, and Oct4 in control and Maf1-induced mESCs and mEBs at day 3. mESCs were differentiated into EBs after infection with either a control lentiviral construct (rtTA) or one expressing an HA epitope-tagged Maf1 construct (Maf1-HA). Control and Maf-HA cells were treated with 1 μg/mL doxycycline (dox) 2 days before formation of mEBs and throughout the process of mEB formation. In (A) and (B), data are mean ± SD of n = 3 independent experiments. Transcript amounts were normalized to β-actin, and the fold change was calculated relative to the amount of transcript in control mESCs. *$p < 0.05$, unpaired Student's t test.

(C) Immunoblot analysis of Maf1-HA, T, and β-actin protein expression in mESCs and mEBs at the indicated days. Protein amounts were normalized to β-actin, and the fold change was calculated relative to the amount of protein in control mESCs.

Maf1 developed visible fat pads (Figures S3C and S3D). Collectively, these results demonstrate a role for Maf1 in promoting adipocyte differentiation.

Inhibition of RNA Pol III-Mediated Transcription Enhances Adipogenesis

As a well-established function of Maf1 is to repress RNA pol III-dependent transcription, we asked whether the observed Maf1-mediated changes in this transcription process contribute to its ability to influence adipocyte differentiation. To do so, we first used an RNA pol III-specific chemical inhibitor, ML-60218 (Wu et al., 2003). Preadipocytes were treated with ML-60218 for 1 day prior to the administration of the differentiation cocktail, and it was removed 2 days later (Figure S1D). A dose-dependent increase in adipogenesis was observed upon inhibitor treatment (Figure S4). At the higher inhibitor concentrations, a modest but reproducible decrease in tRNA gene transcripts was initially observed with ML-60218 treatment, but there was no difference in the amount of these transcripts in the terminally differentiated cells treated with ML-60218 compared with control untreated cells (Figure 6A). Inhibitor treatment resulted in enhanced expression of PPARγ, C/EBPα, and FABP4 mRNA and protein (Figures 6A and 6B) corresponding to an increase in adipocyte formation (Figure 6C). To verify these results, a second approach was used to repress RNA pol III-dependent transcription. Downregulation of Brf1, an RNA pol III-specific TFIIIB transcription factor subunit (Figure S1E), in the 3T3-L1 cells produced a decrease in tRNA transcripts prior to differentiation but not after differentiation of the cells (Figure 6D). Decreases in Brf1 expression resulted in enhanced induction of the pro-adipogenic genes and adipocyte formation (Figures 6E and 6F). We further examined whether these results could be recapitulated in primary cells. Mouse subcutaneous inguinal fat was isolated, and cells obtained from the stromal vascular fraction (SVF) were examined for their ability to differentiate into adipocytes (Figures S1F and S1G). Treatment with ML-60218 enhanced adipocyte formation, as did transfection of these cells with Brf1 small interfering RNAs (siRNAs) to knock down Brf1 expression (Figures S5A–S5D). Our collective results support the idea that at least one mechanism by which Maf1 functions to stimulate adipogenesis is through its ability to repress RNA pol III-dependent transcription.

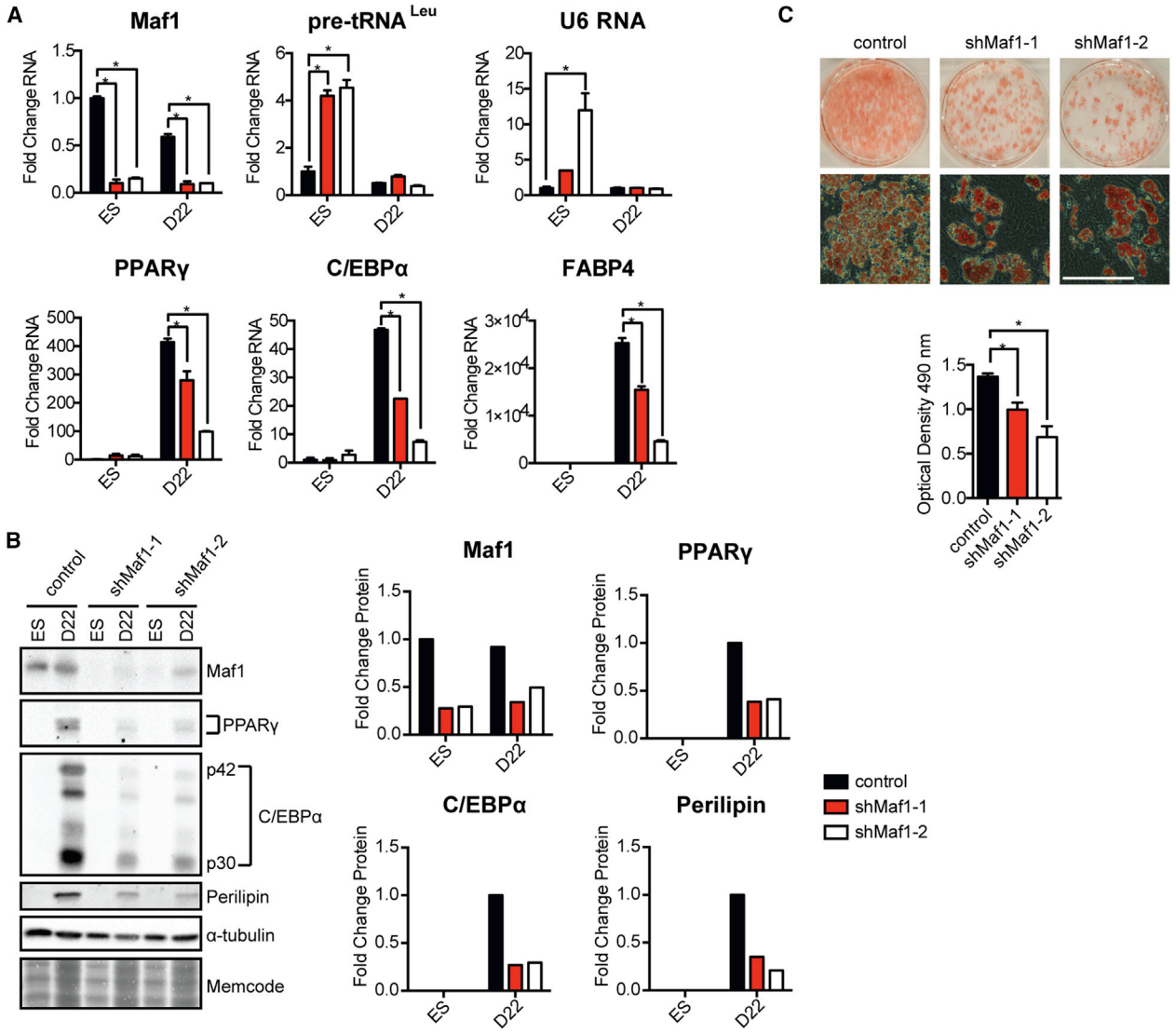

Figure 3. Maf1 Knockdown Compromises Adipogenesis in mESCs

Control and Maf1-knockdown mESCs were terminally differentiated into adipocytes following a standard protocol (Figure S1A).

(A) qRT-PCR analysis depicting expression of $tRNA^{Leu}$, U6 RNA, and mRNA for Maf1, PPARγ, C/EBPα, and their target, FABP4, pre- and post-differentiation of mouse mESCs into adipocytes at day 22 (D22). Transcript amounts were normalized to β-actin, and the fold change was calculated relative to the amount of transcript in control mESCs. Cells were infected with lentivirus harboring Maf1 shRNA-1, Maf1 shRNA-2, or a lentivirus that lacks the Maf1 shRNA. Data are mean ± SD of n = 3 independent experiments. *$p < 0.05$, unpaired Student's t test.

(B) Immunoblot analysis for Maf1, PPARγ, C/EBPα, and perilipin in ESCs and at D22 after differentiation (left) and quantification of changes in protein (right). Fold change in Maf1 expression with Maf1 shRNAs was calculated relative to the expression in ESCs, whereas fold change in PPARγ, C/EBPα, and perilipin with Maf1 knockdown was calculated relative to that at D22.

(C) Representative example of oil red O staining of adipocytes differentiated from control and Maf1-knockdown mESCs (left). Scale bar denotes 200 μm. Quantification of staining (right) represents mean ± SD of n = 3 independent experiments. *$p < 0.05$, unpaired Student's t test.

Altered Maf1 Expression Produces a Distinct Gene Expression Signature Compared with Inhibition of RNA Pol III-Dependent Transcription by Inhibitor Treatment or Brf1 Knockdown

Because our results indicated that changes in RNA pol III-dependent transcription alter cellular mRNA expression, specifically PPARγ and C/EBPα, to enhance adipogenesis, we further determined how Maf1 might regulate PPARγ expression or activity. Ectopic expression of PPARγ in 293T cells was used to analyze PPARγ-mediated transactivation of a promoter containing PPARγ-binding elements (Figure S6). These results revealed that Maf1 does not affect the ability of PPARγ to stimulate transcription in the presence or absence of rosiglitazone, a PPARγ agonist, indicating that Maf1 does not directly regulate PPARγ activity. To further identify other Maf1- and RNA pol III-mediated changes in gene expression that control

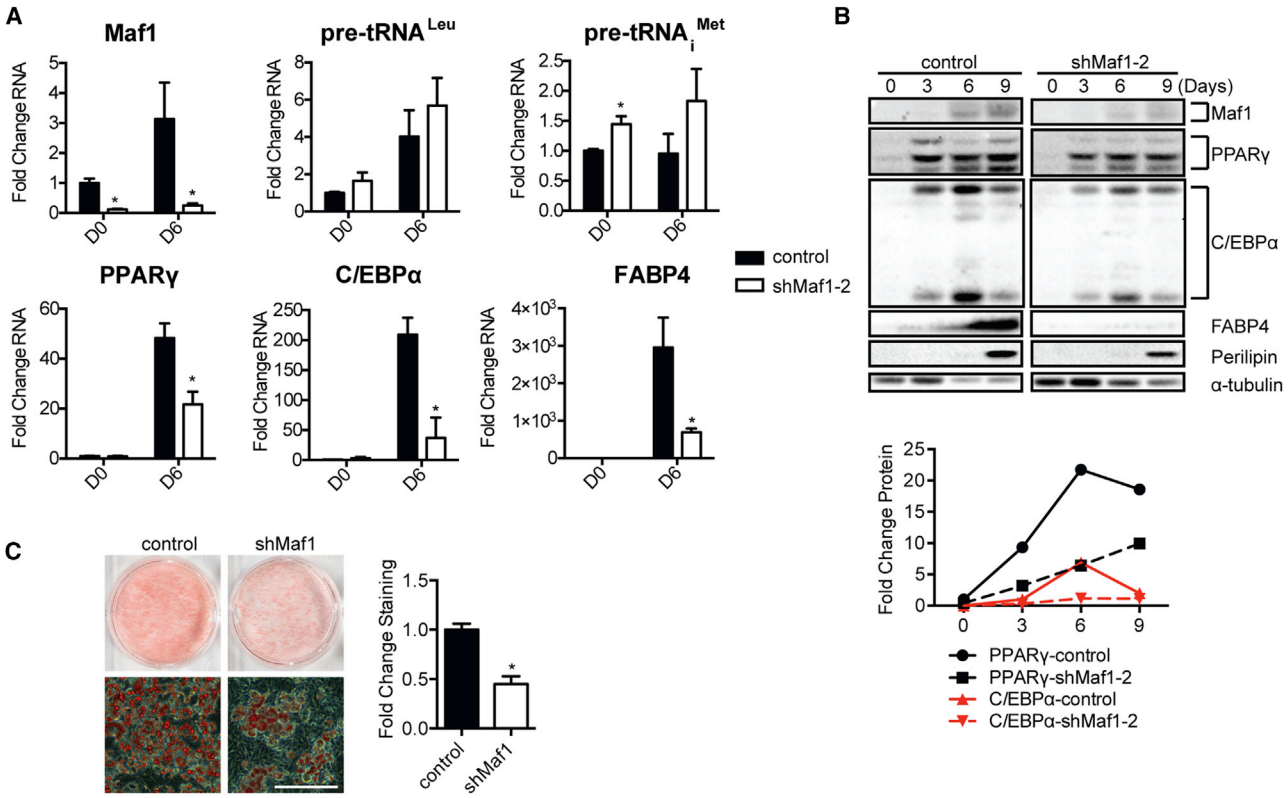

Figure 4. Maf1 Knockdown Reduces Adipogenesis in 3T3-L1 Cells

Maf1 expression was decreased in 3T3-L1 cells using the lentiviral Maf1 shRNA-2 construct. Lentivirus containing no Maf1 shRNA (control) or Maf1 shRNA-2 (knockdown) was used to infect 3T3-L1 cells, and the cells were terminally differentiated into adipocytes using a standard protocol (Figure S1B).

(A) qRT-PCR analysis for expression of Maf1, $tRNA^{Leu}$, $tRNA_i^{Met}$, PPARγ, C/EBPα, and FABP4, pre-differentiation at day 0 (D0) and post-differentiation at day 6 (D6). Transcript amounts were normalized to β-actin, and the fold change was calculated relative to the amount of transcript in day 0 control cells. Data are mean ± SD of n = 3 independent experiments. *$p < 0.05$, unpaired Student's t test.

(B) Immunoblot analysis of Maf1, PPARγ, C/EBPα, FABP4, perilipin, and α-tubulin in control and Maf1-knockdown 3T3-L1 cells at the indicated days. Quantification of expression changes for each of the indicated proteins from the immunoblots is shown (right). Protein amounts were normalized to α-tubulin, and the fold change was calculated relative to the amount of protein in D0 control 3T3-L1 cells.

(C) Oil red O staining of adipocytes differentiated from control and Maf1-knockdown 3T3-L1 cells (left). Scale bar denotes 200 μm. Quantification of staining (right); data represent mean ± SD of n = 3 independent experiments. *$p < 0.05$, unpaired Student's t test.

adipogenesis in 3T3-L1 cells, RNA-seq analysis was conducted. Confluent cells were plated and harvested prior to the addition of the differentiation cocktail (day 0) or 2 days after its addition (day 2). Changes in gene expression produced by Maf1 knockdown (shMaf1), Brf1 knockdown (shBrf1), or ML-60218 (ML) treatment were first analyzed prior to the addition of the differentiation cocktail. shMaf1 produced 1,108 differentially regulated transcripts, while RNA pol III-compromised cells (shBrf1 cells and cells treated with ML-60218) showed only a few genes with changed expression (Figure 7A, top). Gene function analyses showed that Maf1-sensitive genes enriched for a distinct, cell cycle-centric biology at day 0 (Table S1). Analysis of the changes in gene expression incurred by Maf1 knockdown that corresponded to reciprocal changes in gene expression by Brf1 knockdown or ML-60218 treatment also revealed that each of these conditions yielded relatively distinct changes in gene expression (Figure 7B, left). Although it is possible that the observed Maf1-specific changes result from its ability to differentially affect the production of RNA pol III-derived transcripts, these discernible Maf1-specific changes in gene expression may result from Maf1 regulating RNA pol II-dependent gene transcription, as evidence supports that mammalian Maf1 can be recruited to certain RNA pol II-dependent promoters (Johnson et al., 2007; Lee et al., 2015; Li et al., 2016; Palian et al., 2014). Genome-wide analysis of Maf1 chromatin occupancy has been problematic, but recent chromatin immunoprecipitation sequencing (ChIP-seq) analysis showed that it is only very weakly enriched at RNA pol II-driven genes compared with what is observed for its binding at RNA pol III-transcribed genes (Orioli et al., 2016). Our results are nevertheless consistent with the idea that in addition to its ability to selectively regulate mRNA expression through repression of RNA pol III-mediated transcription, Maf1 is capable of regulating mRNA expression in a manner that is distinct from its role in repressing genes that are directly transcribed by RNA pol III.

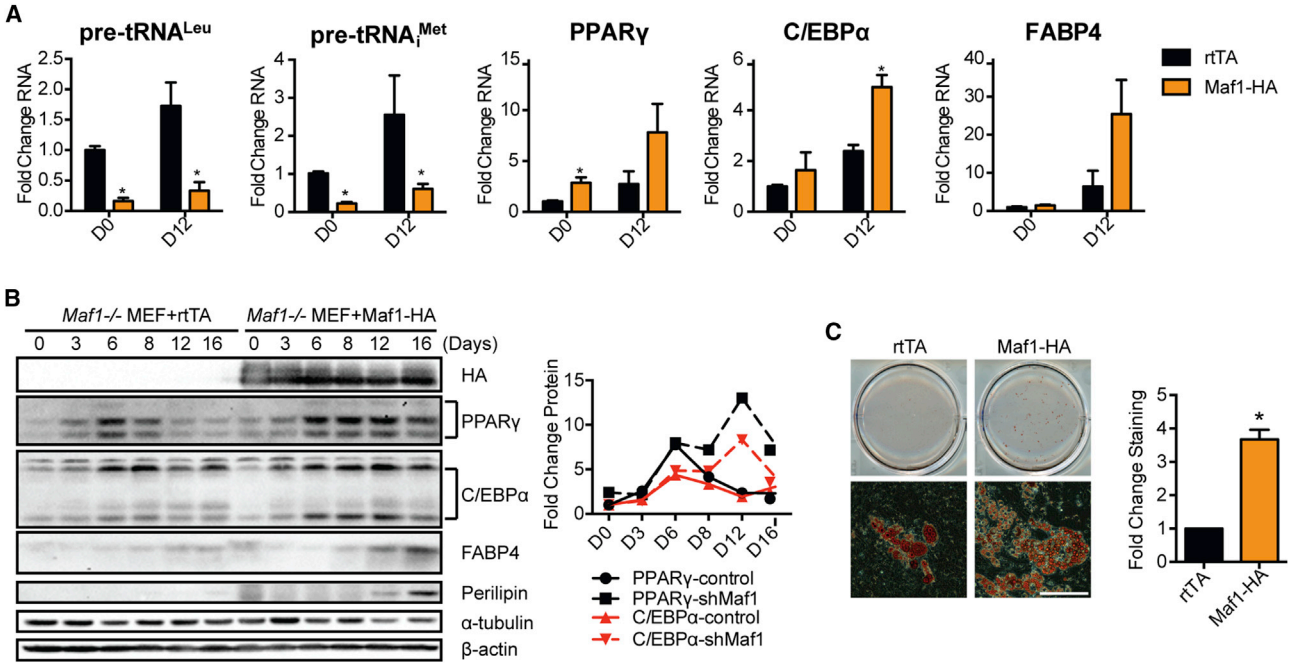

Figure 5. Ectopic Expression of Maf1 Induces Adipogenesis in *Maf1*$^{-/-}$ MEFs

Maf1$^{-/-}$ MEFs were infected with dox-inducible rtTA construct as control (rtTA) or co-infected with both rtTA and Maf1-HA dox-inducible constructs. Control and Maf1-HA expressed *Maf1*$^{-/-}$ MEFs were terminally differentiated into adipocytes using a standard protocol (Figure S1C).

(A) qRT-PCR analysis of RNA expression of tRNA^{Leu}, tRNA$_i^{Met}$, PPARγ, C/EBPα, and FABP4 during the differentiation of either control or Maf1-HA cells that were all treated with 50 ng/mL dox from day 0 (D0) to day 12 (D12). Transcript amounts were normalized to β-actin, and the fold change was calculated relative to the amount of transcript at D0 rtTA *Maf1*$^{-/-}$ MEF cells. Data are mean ± SD of n = 3 independent experiments. *p < 0.05, unpaired Student's t test.

(B) Immunoblot analysis of HA-tagged Maf1, PPARγ, C/EBPα, FABP4, perilipin, and β-actin in control and Maf1 expressed *Maf1*$^{-/-}$ MEF cells. Quantification of the changes in protein expression from the immunoblots is shown (right). Protein amounts were normalized to α-tubulin, and the fold change was calculated relative to the amount of protein in D0 rtTA control *Maf1*$^{-/-}$ MEF cells.

(C) Oil red O staining of adipocytes that are differentiated from control and Maf1-HA expressed *Maf1*$^{-/-}$ MEFs (left). Scale bar denotes 200 μm. Quantification of staining (right); data are mean ± SD of n = 3 independent experiments. *p < 0.05, unpaired Student's t test.

Altered Maf1 Expression and RNA Pol III Transcription Repression during Adipogenesis Produce Overlapping Gene Signatures for Adipocyte Differentiation and Lipid Metabolism

Gene expression analysis at 2 days following the addition of the differentiation cocktail revealed that all samples displayed robust numbers of differentially regulated transcripts (Figure 7A, bottom). Maf1 knockdown-mediated changes indicate that the enrichments at day 2 were different from the biology indicated at day 0, prior to the addition of the differentiation cocktail (Table S1). Although all three conditions affected the production of RNA pol III-derived transcripts, there were both overlapping and distinct sets of genes that were altered by Maf1 knockdown, Brf1 knockdown, and ML-60218 treatment during adipogenesis (Figure 7B, right). Maf1 downregulation altered the expression of genes involved in lipid and sugar metabolism that overlaps with RNA pol III-compromised 3T3-L1 cells undergoing differentiation (Table S2). Enriched gene function analyses were conducted using major databases for gene-function associations and gene signatures. This revealed that shMaf1 downregulated transcripts that were concurrently upregulated by shBrf1 and ML-60218 treatment enriched for fat cell differentiation, lipid metabolism, glucose homeostasis, PPARγ, and adipocytokine signaling pathways. This gene signature after 2 days of cell differentiation overlapped with hallmark gene set enrichment analysis (GSEA) gene sets of adipogenesis and of fatty acids metabolism (Table S2).

RNA Pol III Regulates Non-coding H19 RNA and Wnt6 Expression

To further validate the RNA pol III-targeted genes in the RNA-seq analysis that contribute to its ability to regulate adipogenesis, we examined two candidate genes, the lnc RNA H19 and Wnt6, both of which were induced by RNA pol III-mediated transcription. Wnt6 is an established negative regulator of adipogenesis through its ability to induce β-catenin signaling (Cawthorn et al., 2012). LncRNA H19, transcribed by RNA pol II (Brannan et al., 1990), was also shown to inhibit adipogenesis in mesenchymal stem cells (MSCs) by inhibiting the expression of class II histone deacetylases (Huang et al., 2016). We confirmed that a significant induction of lncRNA H19 expression by Maf1 knockdown was observed both before and after the addition of the differentiation cocktail, whereas RNA pol III-compromised cells displayed a decrease in lncRNA H19 expression (Figure 7C). This indicates that changes in RNA pol III-mediated transcription alter the

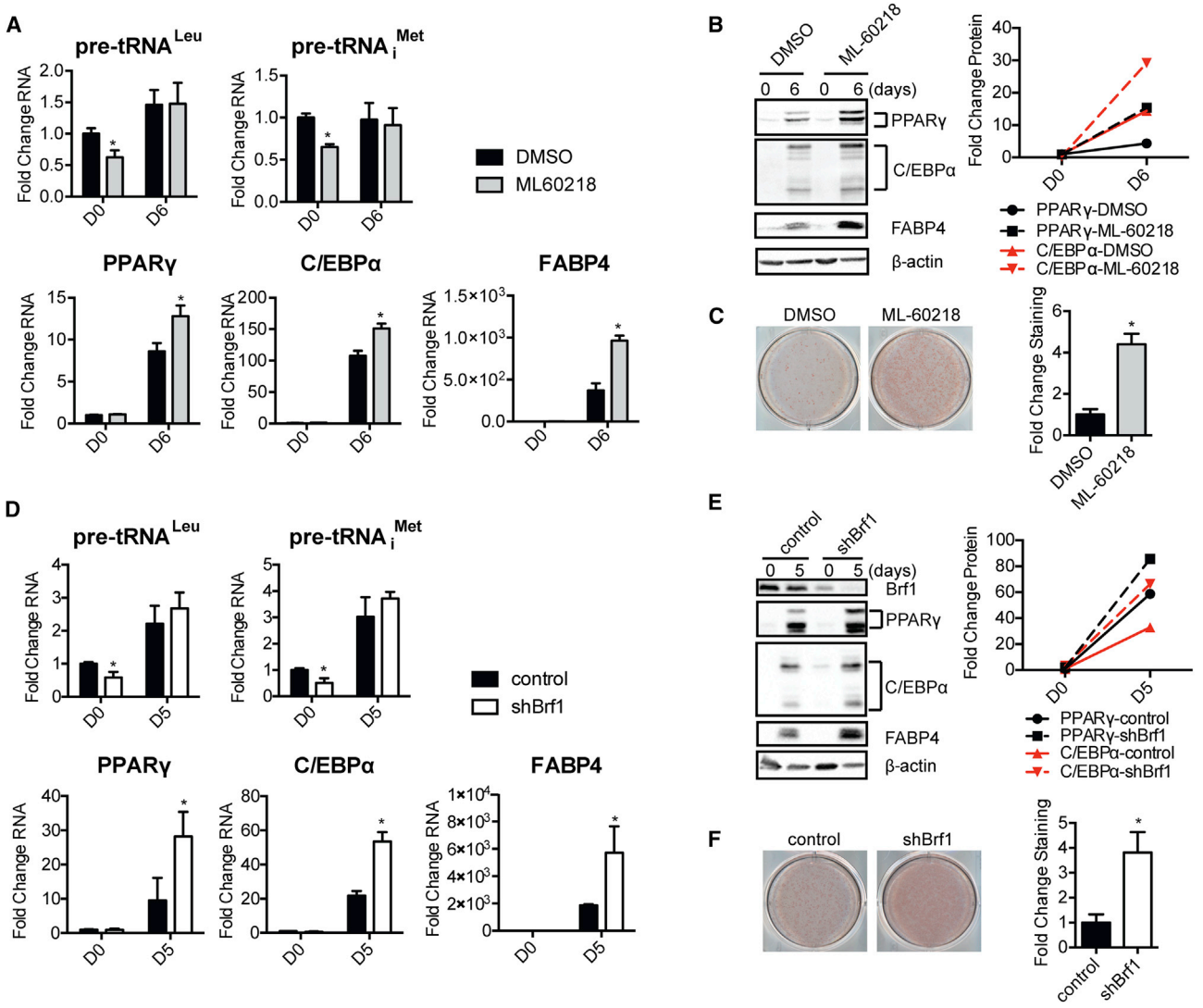

Figure 6. Repression of RNA Pol III-Dependent Transcription by Either ML-60218 Treatment or Brf1 Knockdown Enhances Adipogenesis in 3T3-L1 Cells

ML-60218-treated and Brf-knockdown 3T3-L1 cells were terminally differentiated into adipocytes using a standard protocol (Figures S1D and S1E).

(A) qRT-PCR analysis of $tRNA^{Leu}$, $tRNA_i^{Met}$, PPARγ, C/EBPα, and FABP4 mRNAs during the differentiation of DMSO control and ML-60218-treated 3T3-L1 cells at day 0 (D0) and day 6 (D6). Cells were treated with 40 μM of ML-60218 from day −1 to day 2. Transcript amounts were normalized to β-actin, and the fold change was calculated relative to the amount of transcript at D0 in control cells.

(B) Immunoblot analysis of PPARγ, C/EBPα, FABP4, and β-actin in DMSO control and ML-60218-treated 3T3-L1 cells (left) and quantification of proteins from the immunoblots (right). Protein amounts were normalized to β-actin, and the fold change was calculated relative to the amount of protein at D0 DMSO control cells.

(C) Oil red O staining of adipocytes differentiated from DMSO control and ML-60218 treated 3T3-L1 cells (left) and quantification of staining (right).

(D) qRT-PCR analysis of $tRNA^{Leu}$, $tRNA_i^{Met}$, PPARγ, C/EBPα, and FABP4 mRNAs at D0 before differentiation and at D5 after differentiation of control and Brf1-knockdown 3T3-L1 cells. Transcript amounts were normalized to β-actin, and the fold change was calculated relative to the amount of transcript at D0 for control cells.

(E) Immunoblot analysis of Brf1, PPARγ, C/EBPα, FABP4, and β-actin in control and Brf1-knockdown 3T3-L1 cells (left) and quantification of immunoblots (right). Protein amounts were normalized to β-actin, and the fold change was calculated relative to the amount of protein in D0 for control cells.

(F) Oil red O staining of adipocytes differentiated from control and Brf1-knockdown 3T3-L1 cells.

In (A), (C), (D), and (F), data are mean ± SD of n = 3 independent experiments. *$p < 0.05$, unpaired Student's t test.

expression of these genes, independent of the adipogenesis process, and are not just a consequence of the cells' undergoing adipocyte differentiation. Similarly, inhibition of RNA pol III also decreased Wnt6 expression whereas Maf1 knockdown induced its expression both before and during the differentiation process (Figure 7D). Thus, RNA pol III-mediated transcription positively regulates both lncRNA H19 and Wnt6 expression.

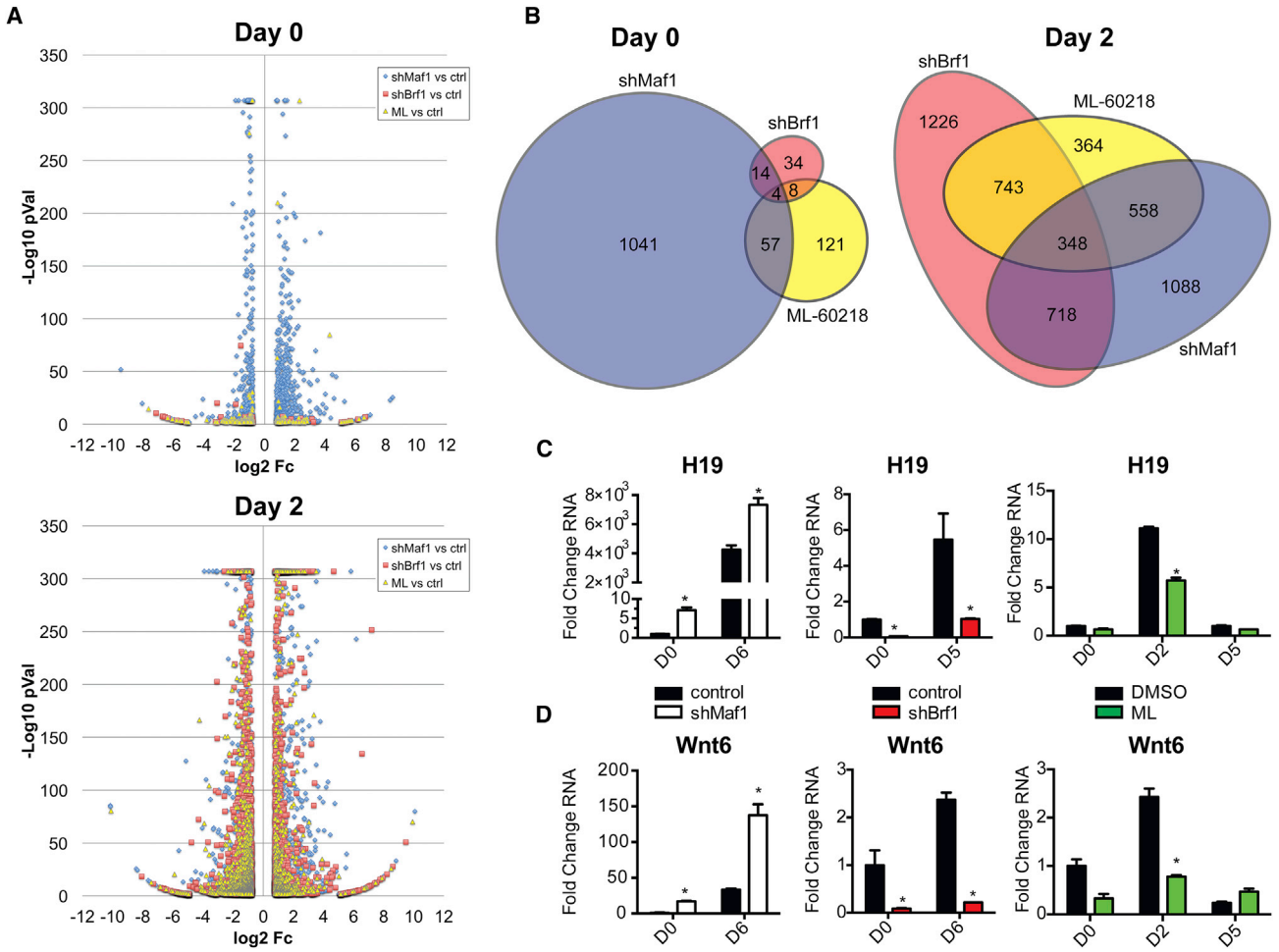

Figure 7. Gene Expression Analysis Shows Distinctiveness in the Maf1 Transcriptome Pre-differentiation and an Enriched Gene Signature for Adipogenic Genes during Differentiation

Differentially regulated transcripts in 3T3-L1 cells that were produced by knockdowns of Maf1, Brf1 (shMaf1 and shBrf1, respectively), or treatment of the cells with the RNA pol III-specific chemical inhibitor ML-60218 (ML).

(A and B) Before addition of differentiation cocktail (day 0) and 2 days after differentiation induction (day 2). (A) Volcano plot illustration of differentially expressed genes selected on the stringency basis of Student's t test p value $\leq$ 0.01 and $\geq$1.7-fold change in expression compared with control cells; they are represented by their fold change in $\log_2$ scale depicted on the x axis and by their statistical significance on the basis of $-\log_{10}$ p value shown on the y axis (transcripts with greater statistical significance are higher in the plot). To limit the height of the illustration, $-\log_{10}$ p values were capped at 307. (B) Area-proportional Euler Venn diagrams of RNA-seq transcripts shown in the volcano plot data where there are 1,108, 52, and 182 differentially regulated genes for shMaf1, shBrf1, and ML-60218, respectively, plotted for day 0 and 2,016, 2,339, and 1,317 genes for day 2.

(C and D) qRT-PCR analysis of expression of lncRNA H19 (C) and Wnt6 (D) in control and Maf1-knockdown, control and Brf1-knockdown, and DMSO control and ML-60218-treated 3T3-L1 cells at the indicated days. Transcript amounts were normalized to β-actin, and the fold change was calculated relative to the amount of transcript at D0 for control cells. *p < 0.05, unpaired Student's t test.

DISCUSSION

Emerging evidence supports the idea that aberrations in RNA pol III and its transcription components can affect human developmental programs. Mutations in RNA pol III subunits are associated with a variety of human developmental diseases, including leukodystrophy (Daoud et al., 2013; Thiffault et al., 2015) and Treacher Collins syndrome (Dauwerse et al., 2011). Mutations in *BRF1*, encoding a TFIIIB transcription factor subunit, were shown to be causal for human cerebellar-facial-dental syndrome (Borck et al., 2015; Jee et al., 2017), whereas mutation in *BDP1*, another TFIIIB subunit, was associated with hereditary hearing loss (Girotto et al., 2013). Several studies have further indicated a role for RNA pol III in cellular differentiation and development. The RNA pol III subunit POLR3G is highly expressed in hESCs compared with differentiated cells (Enver et al., 2005), and its decreased expression results in a loss of hESC pluripotency and the formation of all three germ layers (Wong et al., 2011). Expression of a splice mutant of the POLR3B subunit in zebrafish led to a disruption in the digestive organ and size reductions in other organs (Yee et al., 2007). Furthermore, deficiency of *rpc9*, another RNA pol III subunit, impaired hematopoietic

stem and progenitor cell development in zebrafish (Wei et al., 2016). How specific changes in RNA pol III-dependent transcription affect these processes remains undetermined.

Our results reveal a role for Maf1, a central repressor of RNA pol III-dependent transcription, in the conversion of mESC to mesoderm. Reduced Maf1 expression in mESCs initiate increases in RNA pol III-mediated transcription and inhibits mesoderm-specific marker gene expression during mEB formation. Previous studies examined the genomic distribution of RNA pol III in mouse and hESCs (Alla and Cairns, 2014; Carrière et al., 2012). The occupancy of RNA pol III in hESCs was found to be a consequence of the more active or permissive chromatin state in these cells (Alla and Cairns, 2014). This was shown to be determined, at least in part, by the expression of the pluripotency transcription factors as well as RNA pol II-mediated activity. In addition, there were more tRNA genes occupied overall by RNA pol III in undifferentiated cells than in more highly differentiated cells. Our results indicate that although there was an initial increase in RNA pol III-derived transcripts as mESCs differentiated into EBs, more highly differentiated adipocytes displayed a decrease in transcript levels compared with that observed in mESCs. Thus, our collective results suggest that dynamic changes in RNA pol III-mediated transcription occur during the commitment of mESCs into the different germ layers and that Maf1 may serve to regulate the activity and genomic distribution of RNA pol III at different stages of differentiation.

Our studies have identified a novel role for Maf1 and RNA pol III-mediated transcription repression in the terminal differentiation of cells into adipocytes. Adipogenesis is controlled by a complex and highly orchestrated gene expression program. In mammalian cells, PPARγ and C/EBPα are considered the key early master regulators of adipogenesis (Rosen et al., 2002; Rosen and MacDougald, 2006). Decreased Maf1 expression impaired both the induction of these adipogenic genes and the ability of these cells to form lipid-producing adipocytes in both mESCs and preadipocytes. Importantly, repression of RNA pol III alone is capable of stimulating adipocyte formation, indicating that the activity of RNA pol III modulates adipogenesis. RNA-seq analysis revealed a substantial overlapping enrichment of genes involved in adipogenesis and fat metabolism that are induced during the differentiation process upon Maf1 knockdown that corresponds to reciprocal changes with Brf1 knockdown or RNA pol III inhibitor, ML-60218, treatment. Interestingly, in addition to the subset of overlapping changes in gene expression observed with Maf1 knockdown, ML-60218 treatment, or Brf1 knockdown, we find distinct changes in gene expression elicited by manipulating RNA pol III-dependent transcription by these three different approaches. Although no analyses to date have examined how various strategies to modulate RNA pol III-dependent transcription might affect the expression of RNA pol II-dependent genes, our results indicate that the use of different approaches to manipulate this process do not necessarily produce uniform changes in gene expression.

Recent studies showed that mice with whole-body deletion of *Maf1* do not exhibit gross phenotypic changes that might be expected with impaired mesoderm induction (Bonhoure et al., 2015). This result suggests that in contrast to what we observed *in vitro* with decreased cellular Maf1 amounts, in the context of a whole-body deletion, total loss of Maf1 may result in compensatory changes, likely compounding its important role in homeostasis. Although there was a significant increase in tRNA precursors in the $Maf^{-/-}$ mice, the mature steady-state levels of tRNAs were comparable with the wild-type mice. These mice do not accumulate hepatic lipids under a high-fat diet to the same extent as wild-type mice. This effect was attributed to the robust increase in tRNA precursors and high demand for nucleotides, creating metabolic inefficiency. This futile cycling of nucleotides and lipids may preclude the ability to observe potential changes in adipocyte formation in this mouse model. In contrast to that observed in the $Maf^{-/-}$ mice, manipulation of Maf1 expression was shown to negatively regulate intracellular lipid accumulation both in *C. elegans* and in mouse liver (Khanna et al., 2014; Palian et al., 2014). Although more studies are needed to understand the complex role of Maf1 in lipid metabolism, the present collective work suggests the idea that Maf1 can modulate the production of mature adipocytes and it also functions to maintain lipid homeostasis.

In addition to PPARγ and C/EBPα, analysis of RNA pol III-regulated genes that contribute to its ability to inhibit adipogenesis revealed an unexpected role for this transcription process in positively controlling RNA pol II-generated transcripts, Wnt6 and lncRNA H19. Wnts play a particularly crucial role in adipogenesis. Wnt ligand activation of β-catenin inhibits adipogenesis by inducing nuclear β-catenin expression and preventing the induction of C/EBPβ, C/EBPα, and PPARγ (Prestwich and Macdougald, 2007). Wnt6 is a potent regulator of MSC fate, and its expression significantly impairs adipocyte formation in both 3T3-L1 preadipocytes and the bone marrow-derived stroma ST2 cell line by repressing PPARγ expression (Cawthorn et al., 2012). We further identified lncRNA H19 as another gene target that is responsive to changes in RNA pol III-mediated transcription. In MSCs, lncRNA H19 expression inhibits adipogenesis (Huang et al., 2016). This occurs, at least in part, through the ability of lncRNA H19, and its encoded miR-675, to downregulate the expression of several class II histone deacetylases. Consistent with its inhibitory role in adipogenesis, we find that repression of RNA pol III-mediated transcription decreased expression of lncRNA H19. Collectively, our studies demonstrate that RNA pol III controls the expression of both coding and non-coding RNAs that negatively regulate adipogenesis. In addition, as Wnts (Prestwich and Macdougald, 2007) and lncRNA H19 (Huang et al., 2016; Liang et al., 2016) also play positive roles in osteoblast differentiation, our results suggests the intriguing idea that RNA pol III-dependent transcription could potentially regulate other cell fate decisions.

As RNA pol III regulates various coding and non-coding RNAs to promote adipogenesis, it is likely that multiple mechanisms are involved in producing these changes. Changes in bona fide RNA pol III transcripts could contribute to the observed changes in mRNAs. Modulation of RNA pol III-derived transcripts involved in RNA pol II transcript processing, splicing, and transcription elongation could lead to the observed changes in mRNA and non-coding RNA expression. Alterations in the population of cellular tRNAs have been recently shown to change cellular growth properties by regulating the translation and stability of select mRNAs on the basis of codon use (Gingold et al., 2014;

Goodarzi et al., 2016). The availability of enzymes that modify tRNAs may further determine the population of functional tRNAs (Arimbasseri et al., 2015; Liu et al., 2016). In addition, recent studies have identified a role for tRNA-derived small RNAs that regulate ribosome biogenesis (Kim et al., 2017). However, the observed RNA pol III-mediated changes in H19 lnc RNA suggest that the regulation of adipogenesis by RNA pol III is not only through changes in tRNAs. RNA pol III-transcribed gene activity has been shown to affect the transcription of RNA pol II-transcribed genes. A positive correlation of actively transcribed RNA pol II genes has been observed with nearby RNA pol III genes or with the recruitment of subsets of RNA pol III transcription components (Woolnough et al., 2015). Recent studies further showed that tRNA genes can organize in clusters via DNA loops that connect distal tRNA genes and RNA pol II-transcribed genes to dynamically coordinate gene activity (Van Bortle et al., 2017). Collectively, alterations in RNA pol III-dependent gene activity can have numerous consequences on the expression of RNA pol II-transcribed mRNA and non-coding RNA transcripts. Their possible contributions to RNA pol III-mediated effects on adipogenesis remain to be tested in future studies.

EXPERIMENTAL PROCEDURES

Further detailed experimental procedures are provided in the Supplemental Information.

Cell Culture

46C mESCs were cultured in Glasgow's modified essential medium (GMEM) supplemented with 15% ESC-qualified fetal bovine serum (FBS), 0.1 mM MEM non-essential amino acids (NEAA), 2 mM GlutaMax, 1 mM sodium pyruvate, 0.1 mM β-mercaptoethanol, 1% penicillin/streptomycin, and 100 U/mL LIF. H9 hESCs were maintained in MEF-conditioned medium consisting of DMEM/F12 supplemented with 20% knockout serum replacement, 0.1 mM MEM NEAA, 0.1 mM β-mercaptoethanol, 1% penicillin/streptomycin, and 4 ng/mL recombinant human FGF2. 3T3-L1 mouse preadipocyte, MEF, and HEK293T cells were maintained in DMEM-HG supplemented with 10% FBS, 2 mM GlutaMax, and 1% penicillin/streptomycin. SVF cells were cultured in DMEM/F12 supplemented with 10% FBS, 2 mM GlutaMax, and 1% penicillin/streptomycin. All cells were cultured in incubators with 5% CO_2 at 37°C.

Production of Lentiviral Constructs

Lentiviral particles were produced as described previously (Palian et al., 2014) and in the Supplemental Information.

In Vitro Differentiation of ESCs

For mouse EB formation, mESCs were dissociated with Accutase. mESCs (150,000 cells/mL) were cultured in mESC medium without LIF in six-well Ultra-Low attachment plates. For human EB formation, hESCs (100,000 cells/mL) were cultured in DMEM/F12 supplemented with 10% FBS in 6-well Ultra-Low attachment plates. For both mouse and human EBs, media were changed every other day.

Differentiation of mESCs, 3T3-L1, MEF, and SVF Cells into Adipocytes

Differentiation conditions of mESCs, 3T3-L1, MEF, and SVF cells into adipocytes are described in the Supplemental Information and Figure S1.

RNA Pol III Inhibitor Treatment

The RNA Pol III chemical inhibitor ML-60218 (Millipore) was dissolved in DMSO at a final concentration of 25 mM. The inhibitor was added to the cells at 20 or 40 μM 1 day before the differentiation cocktail was added and removed 2 days later. The control cells were treated with an equal volume of DMSO.

RNA Isolation and Real-Time qPCR

Total RNA was isolated from cells using the Zymo Directzol RNA Kit. The RNAs were then reverse-transcribed into cDNA with the Superscript III first strand synthesis kit (Invitrogen). Real-time qPCR was performed on the LightCycler 480 (Roche) with the SYBR fast qPCR kit (KAPA Biosystems). Relative amount of transcripts were quantified by comparative threshold cycle method (ΔΔCt) with GAPDH or β-actin as the endogenous reference control. The primers for targets are listed in Table S3.

Statistical Analysis

For statistical analysis, unpaired, two-tailed Student's t tests were used for all comparisons of RNA and oil red O analyses. All results are from three biological and two technical replicates. The fold changes were calculated using controls as described in the figure legends.

Immunoblot Analysis and Antibodies

Cells were washed with DPBS twice, then scrapped and pelleted at 400 × *g* for 5 min. The cells were lysed in triple lysis buffer (50 mM Tris-Cl [pH 8.0], 150 mM sodium chloride, 0.02% w/v sodium azide, 1% w/v SDS, 1% v/v NP-40, and 0.5% w/v sodium deoxycholate, containing protease inhibitor cocktail set III; EMD Millipore) for 20 min on ice and sonicated for 15 s. After sonication, the cells were centrifuged for 20 min at 10,000 × *g*, and the supernatant was collected. The protein concentration was determined by using the Bio-Rad Protein *Dc* assay. Cell lysates were subjected to immunoblot analysis and transferred onto a nitrocellulose membrane (GE Healthcare). Membranes were probed using the following antibodies: Maf1 (Abgent), PPARγ, C/EBPα, FABP4, perilipin (Cell Signaling), HA (Roche), T (Santa Cruz), Brf1 (Bethyl), β-actin (Sigma-Aldrich), and α-tubulin (Invitrogen). Protein bands were quantified using Image Lab software (Bio-Rad).

RNA-Seq and Data Analysis

Purified RNA was processed for RNA-seq analysis and sent to EA|Q2 Solutions for library preparation and sequencing. Samples were prepared and sequenced according to a standard TS Stranded mRNA sequencing protocol using HiSeq-Sequencing-2x50bp-PE sequencing on an Illumina sequencing platform. RNA samples were converted into cDNA libraries using the Illumina TruSeq Stranded mRNA sample preparation kit (Illumina). Data analysis of RNA-seq is described in the Supplemental Information.

De Novo Adipogenesis of 3T3-L1 Cells *In Vivo*

For the *de novo* fat pad formation, the above-described control (pLKO.1-empty vector) and Maf1-knockdown (pLKO.1 Maf1 shRNA-2) 3T3-L1 cells were first grown to confluency. The 1 day post-confluent cells were then trypsinized, and 5 × 10^6 cells (per mouse) were spun down at 250 × g for 5 min and resuspended in 200 μL plain DMEM-HG medium. The cell suspensions were injected subcutaneously over the sternum of 8-week-old male athymic mice (The Jackson Laboratory) (institutional protocol #AN-7016). After 8 weeks, the mice were euthanized, and the skin covering the sternum was examined for the presence of a fat pad. The skin pieces containing fat pads were fixed in neutral-buffered formalin, sectioned cross-wise, and stained with H&E.

DATA AND SOFTWARE AVAILABILITY

The accession number for the RNA-seq data reported in this paper is GEO: GSE113324.

SUPPLEMENTAL INFORMATION

Supplemental Information includes Supplemental Experimental Procedures, six figures, and three tables and can be found with this article online at https://doi.org/10.1016/j.celrep.2018.07.046.

ACKNOWLEDGMENTS

This work was supported by NIH grants CA108614 and CA74138 to D.L.J. We would like to thank Dr. Charles Foulds and Dr. Sean Hartig for helpful

discussions and Dr. Aleksandra Rusin for her excellent assistance with the mouse experiments and analyses.

AUTHOR CONTRIBUTIONS

Methodology, C.-Y.C., R.B.L., W.L., and D.L.J.; Validation, C.-Y.C., C.J.W., and W.-H.C.; Formal Analysis, C.-Y.C. and R.B.L.; Investigation, C.-Y.C., R.B.L., and C.J.W.; Resources, W.-H.C. and W.L.; Writing – Original Draft, C.-Y.C., R.B.L., and D.L.J.; Writing – Review & Editing, C.-Y.C., R.B.L., C.J.W., and D.L.J.; Visualization, C.-Y.C., R.B.L., and D.L.J.; Supervision, C.-Y.C. and D.L.J.; Funding Acquisition, D.L.J.

DECLARATION OF INTERESTS

The authors declare no competing interests.

Received: December 15, 2017
Revised: April 5, 2018
Accepted: July 12, 2018
Published: August 14, 2018

REFERENCES

Alla, R.K., and Cairns, B.R. (2014). RNA polymerase III transcriptomes in human embryonic stem cells and induced pluripotent stem cells, and relationships with pluripotency transcription factors. PLoS ONE *9*, e85648–e85617.

Arimbasseri, A.G., Blewett, N.H., Iben, J.R., Lamichhane, T.N., Cherkasova, V., Hafner, M., and Maraia, R.J. (2015). RNA polymerase III output is functionally linked to tRNA dimethyl-G26 modification. PLoS Genet. *11*, e1005671.

Baenke, F., Peck, B., Miess, H., and Schulze, A. (2013). Hooked on fat: the role of lipid synthesis in cancer metabolism and tumour development. Dis. Model. Mech. *6*, 1353–1363.

Boguta, M., Czerska, K., and Zoładek, T. (1997). Mutation in a new gene MAF1 affects tRNA suppressor efficiency in Saccharomyces cerevisiae. Gene *185*, 291–296.

Bonhoure, N., Byrnes, A., Moir, R.D., Hodroj, W., Preitner, F., Praz, V., Marcelin, G., Chua, S.C., Jr., Martinez-Lopez, N., Singh, R., et al. (2015). Loss of the RNA polymerase III repressor MAF1 confers obesity resistance. Genes Dev. *29*, 934–947.

Borck, G., Hög, F., Dentici, M.L., Tan, P.L., Sowada, N., Medeira, A., Gueneau, L., Holger, T., Kousi, M., Lepri, F., et al. (2015). BRF1 mutations alter RNA polymerase III-dependent transcription and cause neurodevelopmental anomalies. Genome Res. *25*, 609.

Brannan, C.I., Dees, E.C., Ingram, R.S., and Tilghman, S.M. (1990). The product of the H19 gene may function as an RNA. Mol. Cell. Biol. *10*, 28–36.

Carrière, L., Graziani, S., Alibert, O., Ghavi-Helm, Y., Boussouar, F., Humbertclaude, H., Jounier, S., Aude, J.C., Keime, C., Murvai, J., et al. (2012). Genomic binding of Pol III transcription machinery and relationship with TFIIS transcription factor distribution in mouse embryonic stem cells. Nucleic Acids Res. *40*, 270–283.

Cawthorn, W.P., Bree, A.J., Yao, Y., Du, B., Hemati, N., Martinez-Santibañez, G., and MacDougald, O.A. (2012). Wnt6, Wnt10a and Wnt10b inhibit adipogenesis and stimulate osteoblastogenesis through a β-catenin-dependent mechanism. Bone *50*, 477–489.

Clarke, C.J., Berg, T.J., Birch, J., Ennis, D., Mitchell, L., Cloix, C., Campbell, A., Sumpton, D., Nixon, C., Campbell, K., et al. (2016). The initiator methionine tRNA drives secretion of type II collagen from stromal fibroblasts to promote tumor growth and angiogenesis. Curr. Biol. *26*, 755–765.

Daoud, H., Tétreault, M., Gibson, W., Guerrero, K., Cohen, A., Gburek-Augustat, J., Synofzik, M., Brais, B., Stevens, C.A., Sanchez-Carpintero, R., et al. (2013). Mutations in POLR3A and POLR3B are a major cause of hypomyelinating leukodystrophies with or without dental abnormalities and/or hypogonadotropic hypogonadism. J. Med. Genet. *50*, 194–197.

Dauwerse, J.G., Dixon, J., Seland, S., Ruivenkamp, C.A., van Haeringen, A., Hoefsloot, L.H., Peters, D.J., Boers, A.C., Daumer-Haas, C., Maiwald, R., et al. (2011). Mutations in genes encoding subunits of RNA polymerases I and III cause Treacher Collins syndrome. Nat. Genet. *43*, 20–22.

Desai, N., Lee, J., Upadhya, R., Chu, Y., Moir, R.D., and Willis, I.M. (2005). Two steps in Maf1-dependent repression of transcription by RNA polymerase III. J. Biol. Chem. *280*, 6455–6462.

Enver, T., Soneji, S., Joshi, C., Brown, J., Iborra, F., Ørntoft, T., Thykjaer, T., Maltby, E., Smith, K., Abu Dawud, R., et al. (2005). Cellular differentiation hierarchies in normal and culture-adapted human embryonic stem cells. Hum. Mol. Genet. *14*, 3129–3140.

Filer, D., Thompson, M.A., Takhaveev, V., Dobson, A.J., Kotronaki, I., Green, J.W.M., Heinemann, M., Tullet, J.M.A., and Alic, N. (2017). RNA polymerase III limits longevity downstream of TORC1. Nature *552*, 263–267.

Gingold, H., Tehler, D., Christoffersen, N.R., Nielsen, M.M., Asmar, F., Kooistra, S.M., Christophersen, N.S., Christensen, L.L., Borre, M., Sørensen, K.D., et al. (2014). A dual program for translation regulation in cellular proliferation and differentiation. Cell *158*, 1281–1292.

Girotto, G., Abdulhadi, K., Buniello, A., Vozzi, D., Licastro, D., d'Eustacchio, A., Vuckovic, D., Alkowari, M.K., Steel, K.P., Badii, R., and Gasparini, P. (2013). Linkage study and exome sequencing identify a BDP1 mutation associated with hereditary hearing loss. PLoS ONE *8*, e80323.

Goodarzi, H., Nguyen, H.C.B., Zhang, S., Dill, B.D., Molina, H., and Tavazoie, S.F. (2016). Modulated expression of specific tRNAs drives gene expression and cancer progression. Cell *165*, 1416–1427.

Huang, Y., Zheng, Y., Jin, C., Li, X., Jia, L., and Li, W. (2016). Long non-coding RNA H19 inhibits adipocyte differentiation of bone marrow mesenchymal stem cells through epigenetic modulation of histone deacetylases. Sci. Rep. *6*, 28897.

Jee, Y.H., Sowada, N., Markello, T.C., Rezvani, I., Borck, G., and Baron, J. (2017). BRF1 mutations in a family with growth failure, markedly delayed bone age, and central nervous system anomalies. Clin. Genet. *91*, 739–747.

Johnson, D.L., and Johnson, S.A.S. (2008). Cell biology. RNA metabolism and oncogenesis. Science *320*, 461–462.

Johnson, S.S., Zhang, C., Fromm, J., Willis, I.M., and Johnson, D.L. (2007). Mammalian Maf1 is a negative regulator of transcription by all three nuclear RNA polymerases. Mol. Cell *26*, 367–379.

Johnson, S.A.S., Dubeau, L., and Johnson, D.L. (2008). Enhanced RNA polymerase III-dependent transcription is required for oncogenic transformation. J. Biol. Chem. *283*, 19184–19191.

Khanna, A., Johnson, D.L., and Curran, S.P. (2014). Physiological roles for mafr-1 in reproduction and lipid homeostasis. Cell Rep. *9*, 2180–2191.

Kim, H.K., Fuchs, G., Wang, S., Wei, W., Zhang, Y., Park, H., Roy-Chaudhuri, B., Li, P., Xu, J., Chu, K., et al. (2017). A transfer-RNA-derived small RNA regulates ribosome biogenesis. Nature *552*, 57–62.

Lee, Y.-L., Li, Y.-C., Su, C.-H., Chiao, C.-H., Lin, I.-H., and Hsu, M.-T. (2015). MAF1 represses CDKN1A through a Pol III-dependent mechanism. eLife *4*, e06283.

Li, Y., Tsang, C.K., Wang, S., Li, X.X., Yang, Y., Fu, L., Huang, W., Li, M., Wang, H.Y., and Zheng, X.F. (2016). MAF1 suppresses AKT-mTOR signaling and liver cancer through activation of PTEN transcription. Hepatology *63*, 1928–1942.

Liang, W.C., Fu, W.M., Wang, Y.B., Sun, Y.X., Xu, L.L., Wong, C.W., Chan, K.M., Li, G., Waye, M.M., and Zhang, J.F. (2016). H19 activates Wnt signaling and promotes osteoblast differentiation by functioning as a competing endogenous RNA. Sci. Rep. *6*, 20121.

Liu, F., Clark, W., Luo, G., Wang, X., Fu, Y., Wei, J., Wang, X., Hao, Z., Dai, Q., Zheng, G., et al. (2016). ALKBH1-mediated tRNA demethylation regulates translation. Cell *167*, 816–828.e6.

Orioli, A., Praz, V., Lhôte, P., and Hernandez, N. (2016). Human MAF1 targets and represses active RNA polymerase III genes by preventing recruitment rather than inducing long-term transcriptional arrest. Genome Res. *26*, 624–635.

Palian, B.M., Rohira, A.D., Johnson, S.A.S., He, L., Zheng, N., Dubeau, L., Stiles, B.L., and Johnson, D.L. (2014). Maf1 is a novel target of PTEN and PI3K signaling that negatively regulates oncogenesis and lipid metabolism. PLoS Genet. *10*, e1004789.

Prestwich, T.C., and Macdougald, O.A. (2007). Wnt/beta-catenin signaling in adipogenesis and metabolism. Curr. Opin. Cell Biol. *19*, 612–617.

Rippon, H.J., and Bishop, A.E. (2004). Embryonic stem cells. Cell Prolif. *37*, 23–34.

Rosen, E.D., and MacDougald, O.A. (2006). Adipocyte differentiation from the inside out. Nat. Rev. Mol. Cell Biol. *7*, 885–896.

Rosen, E.D., Hsu, C.H., Wang, X., Sakai, S., Freeman, M.W., Gonzalez, F.J., and Spiegelman, B.M. (2002). C/EBPalpha induces adipogenesis through PPARgamma: a unified pathway. Genes Dev. *16*, 22–26.

Thiffault, I., Wolf, N.I., Forget, D., Guerrero, K., Tran, L.T., Choquet, K., Lavallée-Adam, M., Poitras, C., Brais, B., Yoon, G., et al. (2015). Recessive mutations in POLR1C cause a leukodystrophy by impairing biogenesis of RNA polymerase III. Nat. Commun. *6*, 7623.

Turowski, T.W., and Tollervey, D. (2016). Transcription by RNA polymerase III: insights into mechanism and regulation. Biochem. Soc. Trans. *44*, 1367–1375.

Upadhya, R., Lee, J., and Willis, I.M. (2002). Maf1 is an essential mediator of diverse signals that repress RNA polymerase III transcription. Mol. Cell *10*, 1489–1494.

Van Bortle, K., Phanstiel, D.H., and Snyder, M.P. (2017). Topological organization and dynamic regulation of human tRNA genes during macrophage differentiation. Genome Biol. *18*, 180.

Wei, Y., Xu, J., Zhang, W., Wen, Z., and Liu, F. (2016). RNA polymerase III component Rpc9 regulates hematopoietic stem and progenitor cell maintenance in zebrafish. Development *143*, 2103–2110.

Wong, R.C., Pollan, S., Fong, H., Ibrahim, A., Smith, E.L., Ho, M., Laslett, A.L., and Donovan, P.J. (2011). A novel role for an RNA polymerase III subunit POLR3G in regulating pluripotency in human embryonic stem cells. Stem Cells *29*, 1517–1527.

Woolnough, J.L., Atwood, B.L., and Giles, K.E. (2015). Argonaute 2 binds directly to tRNA genes and promotes gene repression in cis. Mol. Cell. Biol. *35*, 2278–2294.

Wu, L., Pan, J., Thoroddsen, V., Wysong, D.R., Blackman, R.K., Bulawa, C.E., Gould, A.E., Ocain, T.D., Dick, L.R., Errada, P., et al. (2003). Novel small-molecule inhibitors of RNA polymerase III. Eukaryot. Cell *2*, 256–264.

Yee, N.S., Gong, W., Huang, Y., Lorent, K., Dolan, A.C., Maraia, R.J., and Pack, M. (2007). Mutation of RNA Pol III subunit rpc2/polr3b Leads to Deficiency of Subunit Rpc11 and disrupts zebrafish digestive development. PLoS Biol. *5*, e312.

Zhao, H., and Jin, Y. (2017). Signaling networks in the control of pluripotency. Curr. Opin. Genet. Dev. *46*, 141–148.

Cell Reports, Volume *24*

Supplemental Information

Maf1 and Repression of RNA Polymerase III-Mediated Transcription Drive Adipocyte Differentiation

Chun-Yuan Chen, Rainer B. Lanz, Christopher J. Walkey, Wen-Hsuan Chang, Wange Lu, and Deborah L. Johnson

SUPPLEMENTAL FIGURES

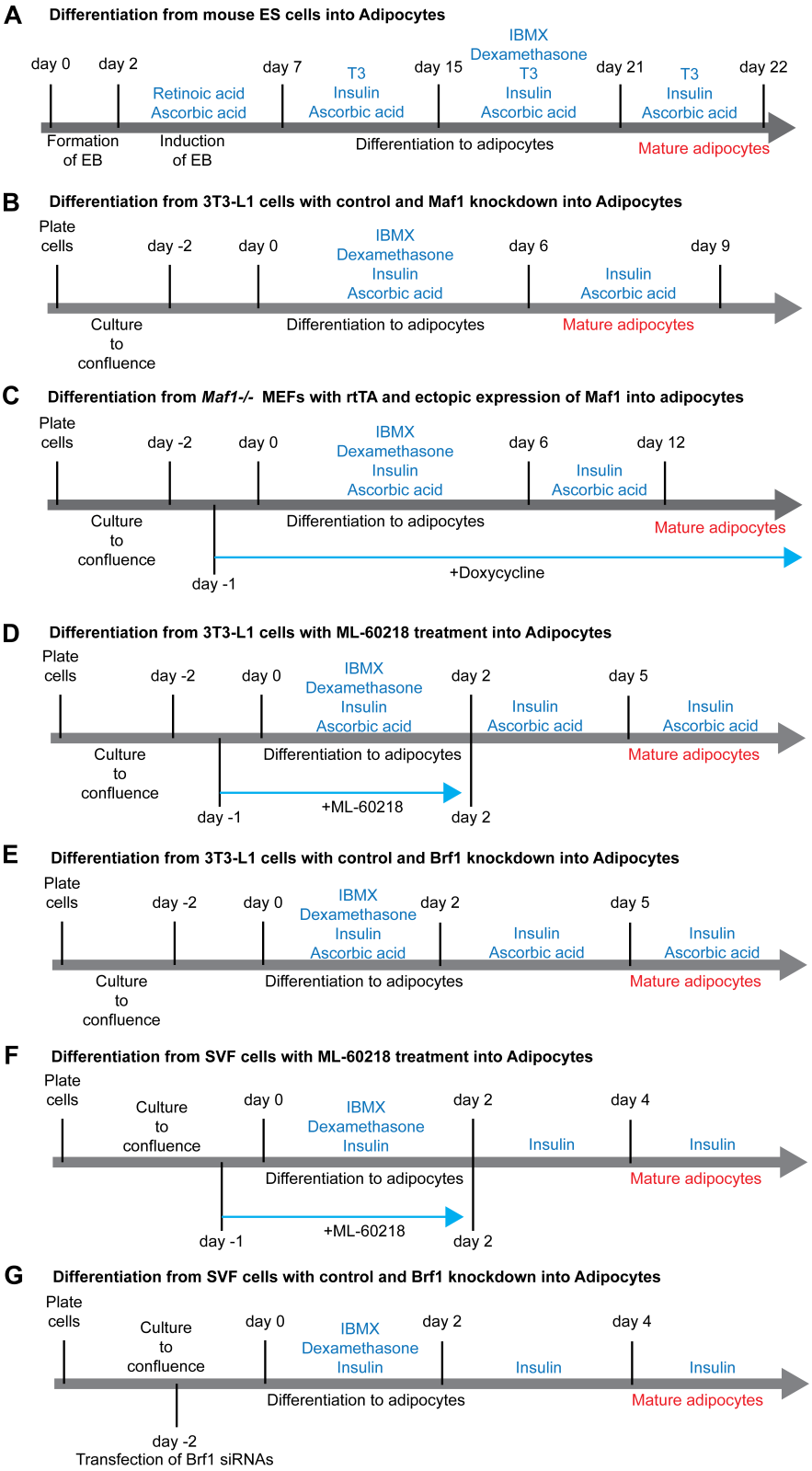

Figure S1: ***Stepwise protocols for the differentiation of mESCs, 3T3-L1 cells, and MEFs into mature adipocytes. Related to Fig. 3-6, S3, and S4.***

The detailed protocols and concentration of each reagent are depicted in the "Methods". **(A)** Differentiation of the control and Maf1 knockdown mESCs into adipocytes. (IBMX, 3-isobutyl-1-methylxanthine; T3, Triiodothyronine) **(B)** Differentiation of the control and Maf1-knockdown 3T3-L1 cells into adipocytes. **(C)** Differentiation of the rtTA control and Maf1-HA expressed *Maf1*-/- MEFs into adipocytes. **(D)** Differentiation of the 3T3-L1 cells with ML-60218 treatment into adipocytes. ML-60218 was added to the cells 24 hours prior the induction of adipogenesis and removed 2 days later. **(E)** Differentiation of the control and Brf1-knockdown 3T3-L1 cells into adipocytes. **(F)** Differentiation of the SVF cells with ML-60218 treatment into adipocytes. ML-60218 was added to the cells 24 hours prior the induction of adipogenesis and removed 2 days later. **(G)** Differentiation of the control and Brf1-knockdown SVF cells into adipocytes.

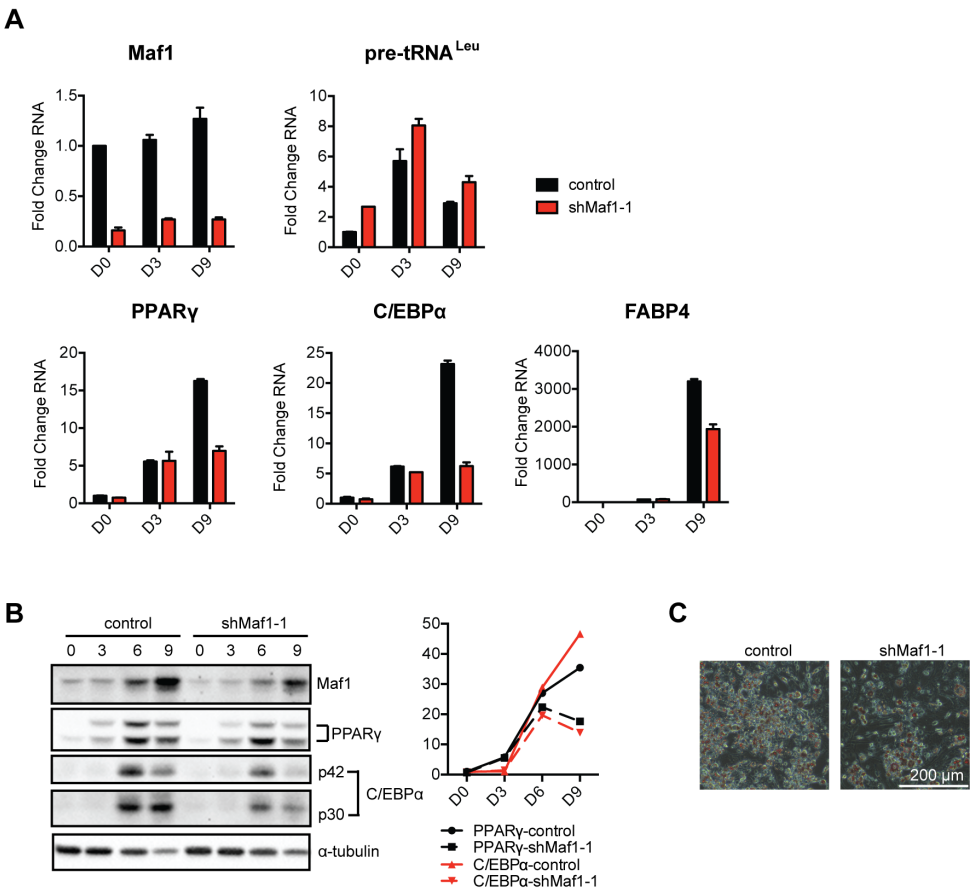

Figure S2: ***Maf1 knockdown reduces adipogenesis in 3T3-L1 cells. Related to Fig. 4.***
Maf1 expression was decreased in 3T3-L1 cells using the lentiviral Maf1 shRNA-1 construct. Lentivirus containing no Maf1 shRNA (control) or Maf1 shRNA-1 (knockdown) was used to infect 3T3-L1 cells, and the cells were terminally differentiated into adipocytes using a standard protocol (Fig. S1B). **(A)** qRT-PCR analysis for expression of Maf1, $tRNA^{Leu}$, PPARγ, C/EBPα, and FABP4. Pre-differentiation at day 0 (D0) and post- differentiation at day 3 (D3) and day 9 (D9). Transcript amounts were normalized to β-actin and the fold change was calculated relative to the amount of transcript in day 0 control cells. **(B)** Immunoblot analysis of Maf1, PPARγ, C/EBPα, and α-tubulin in control and Maf1 knockdown 3T3-L1 cells at the indicated days. Quantification of expression changes for each of the indicated proteins from the immunoblots is shown (right). Protein amounts were normalized to α-tubulin and the fold change was calculated relative to the amount of protein in D0 control 3T3-L1 cells. **(C)** Oil-red O staining of adipocytes differentiated from control and Maf1 knockdown 3T3-L1 cells.

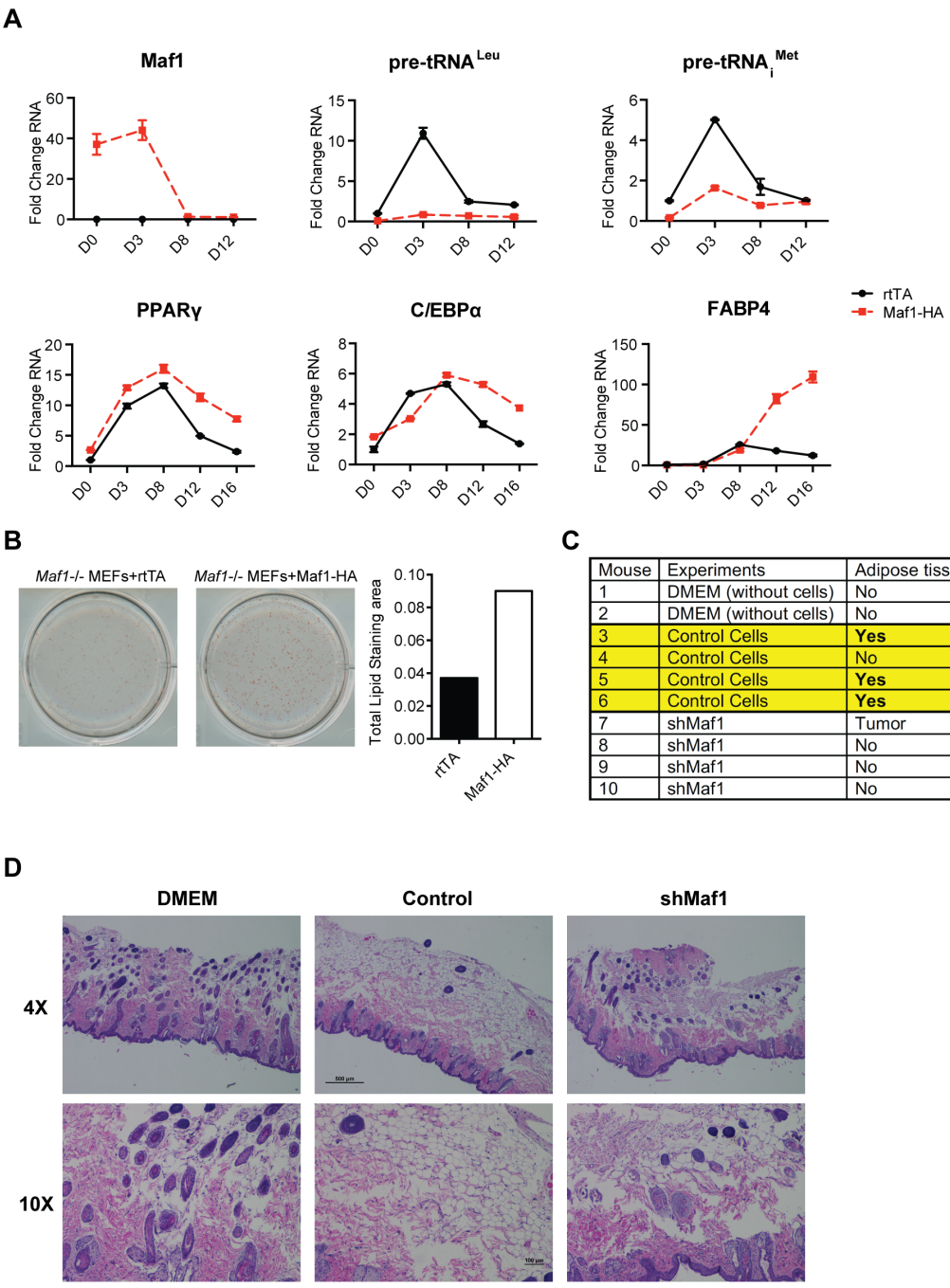

Mouse	Experiments	Adipose tissue observed
1	DMEM (without cells)	No
2	DMEM (without cells)	No
3	Control Cells	**Yes**
4	Control Cells	No
5	Control Cells	**Yes**
6	Control Cells	**Yes**
7	shMaf1	Tumor
8	shMaf1	No
9	shMaf1	No
10	shMaf1	No

Figure S3: ***Maf1 promotes adipogenesis in vitro and in vivo. Related to Fig. 4-5.***
(A, B) Induction of Maf1 at the early stage of adipogenesis is sufficient to promote the adipogenesis in Maf1-/- MEFs. The rtTA control and Maf1-HA expressed *Maf1-/-* MEFs were programmed to differentiate into adipocytes, and treated with 50 ng/ml dox only from day -1 to day 3. **(A)** qRT-PCR analysis of RNA expression of Maf1, $tRNA^{Leu}$, $tRNA_i^{Met}$, PPARγ, C/EBPα, and FABP4 during the differentiation of either control or Maf1-HA expressed *Maf1-/-* MEFs at the indicated days. Transcript amounts were normalized to β-actin and the fold change was calculated relative to the amount of transcript at day 0 (D0) rtTA *Maf1-/-* MEF cells. **(B)** Oil-red O staining of adipocytes that are differentiated from control and Maf1-HA expressed *Maf1 -/-* MEFs (left) and quantification of staining (right). **(C, D)** Reduction of Maf1 compromises the fat pad formation of implanted 3T3-L1 preadipocytes. (C) For the de novo adipogenesis of 3T3-L1 cells in vivo, 10 mice were used. Two mice were injected with plain DMEM medium with no cells as negative controls. Four mice were injected with 3T3-L1 control cells (empty

vector), three out of four developed a visible fat pads in the injected region. The other four mice were injected with Maf1 knockdown 3T3-L1 cells, none of them developed a visible fat pad. **(D)** H&E stained skin cross-sections from the mice that were injected with DMEM, and control and Maf1 knockdown (shMaf1) 3T3-L1 cells. The pictures were taken under microscope with two magnifications, 4X and 10X, of each sample.

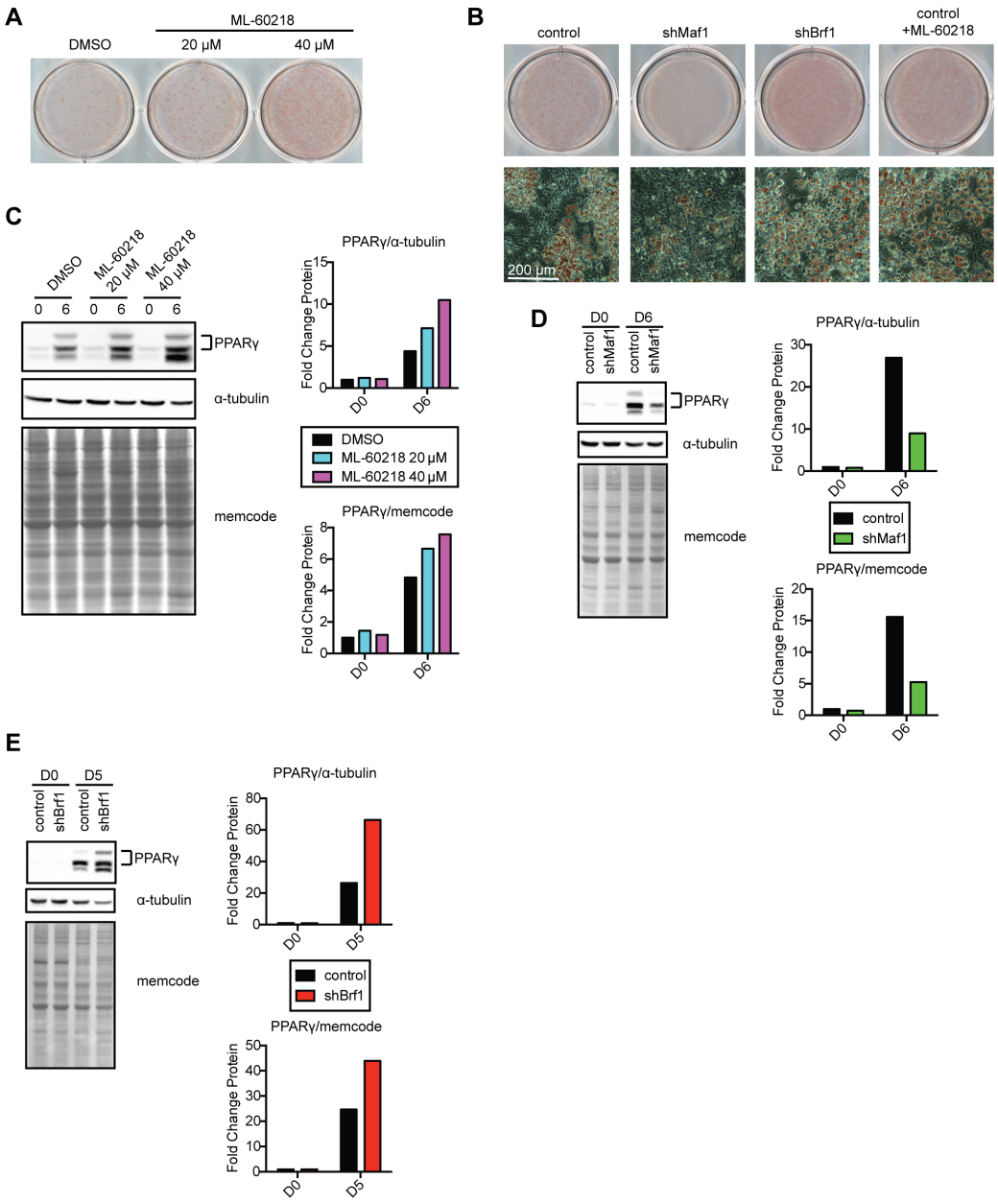

Figure S4: ***Repression of RNA Pol III-dependent transcription by either ML-60218 treatment or Brf1 knockdown promotes adipogenesis in 3T3-L1 cells. Related to Fig. 4 and 6.***

(A) Dose dependent increase of adipogenesis in 3T3-L1 cells with ML-60218 treatment. 3T3-L1 cells were treated with DMSO, and 20 μM or 40 μM of ML-60218 from day -1 to day 2 relative to inclusion of the differentiation cocktailand the cells were fixed at day 6 for Oil-red O staining. **(B)** Maf1 knockdown represses adipogenesis, whereas both Brf1 knockdown and ML-60218 treatment enhances adipogenesis compare to control cells. 40 μM of ML-60218 were treated to the cells from day -1 to day 2, and the all the cells were fixed at day 5 for Oil-red O staining. **(C-E)** Immunoblot analysis of PPARγ and α-tubulin (left) in **(C)** DMSO control and 20 μM or 40 μM ML-60218 treated 3T3-L1 cells; **(D)** control and Maf1-knockdown 3T3-L1 cells; **(E)** control and Brf1-knockdown 3T3-L1 cells, and the quantification of proteins from the immunoblots (right). Protein amounts were normalized to α-tubulin and total protein (memcode), and the fold change was calculated relative to the amount of protein at D0 DMSO control cells.

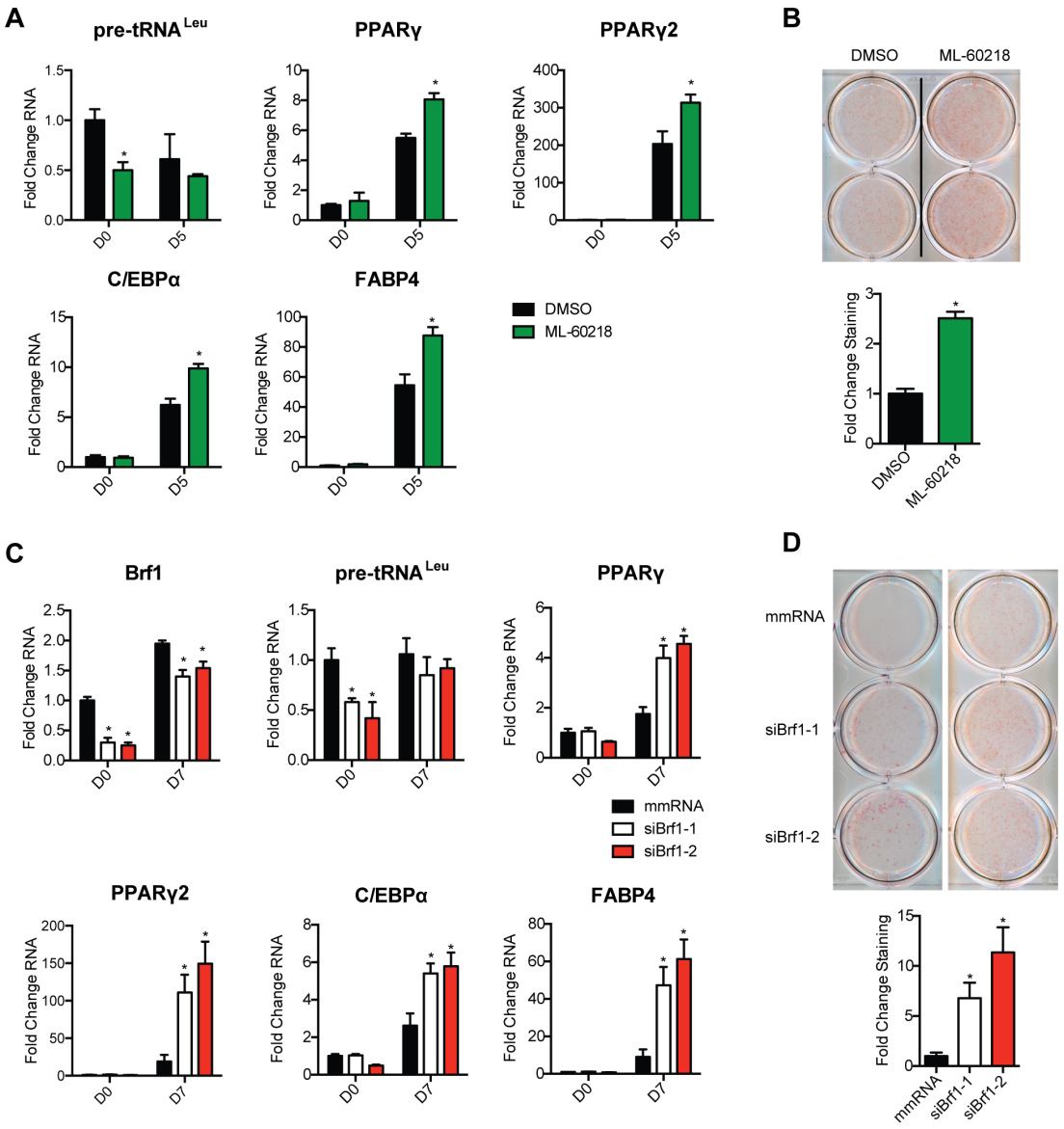

Figure S5: ***Repression of RNA pol III-dependent transcription by either ML-60218 treatment or Brf1 knockdown promotes adipogenesis in primary mouse SVF cells. Related to Fig. 6.***

(A) ML-60218-treated and Brf-knockdown mouse SVF cells were terminally differentiated into adipocytes using a standard protocol (Fig. S1F-G). (A) qRT-PCR analysis of $tRNA^{Leu}$, and PPARγ, C/EBPα, and FABP4 mRNAs during the differentiation of DMSO control and ML-60218-treated SZVF cells at Day 0 and Day 5 (D0 and D5). Cells were treated with 20 μM of ML-60218 from day -1 to day 2. Transcript amounts were normalized to PPia1 and the fold change was calculated relative to the amount of transcript at D0 in control cells. **(B)** Oil-red O staining of adipocytes differentiated from DMSO control and ML-60218 treated SVF cells (Top) and quantification of staining (Bottom). **(C)** qRT-PCR analysis of $tRNA^{Leu}$, and PPARγ, C/EBPα, and FABP4 mRNAs at day 0 (D0) before differentiation and at day 7 (D7) after differentiation of control mismatched RNA (mmRNA) and Brf1-knockdown with two different siRNAs in SVF cells. Transcript amounts were normalized to PPia1 and the fold change was calculated relative to the amount of transcript at D0 for control cells. **(D)** Oil-red O staining of adipocytes differentiated from mmRNA and Brf1-knockdown SVF cells. **(A-D)** Data are mean ± s.d. of n=3 independent experiments. Asterisks represent $p<0.05$ in an unpaired Student's t test.

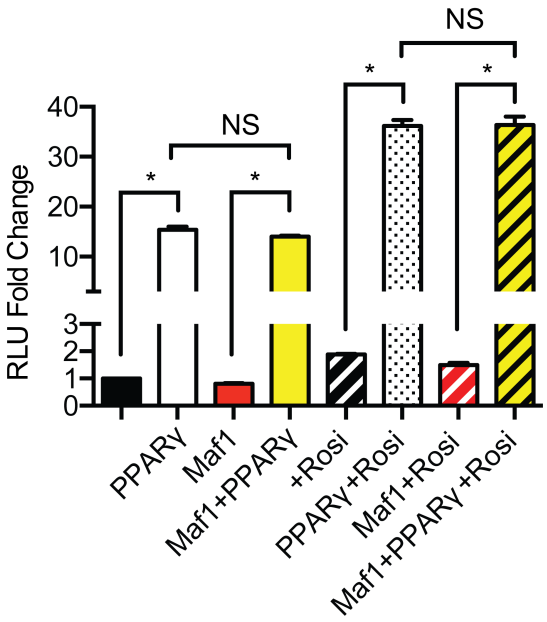

Figure S6: ***Maf1 does not affect the PPARγ transcription activity. Related to Fig 7.***
293T cells were co-transfected with either PPARγ or Maf1-HA or both, and a luciferase reporter containing PPARγ-response element and Renilla, with and without the treatment of rosiglitazone (1μM). Luciferase activity was measured from resulting lysates and normalized to Renilla luciferase activity; fold change was calculated relative to the luciferase activity in control cells without PPARγ and Maf1-HA expression. Values shown are the means ± s.d. of n=4 independent experiments. Asterisks represent $p<0.05$ in an unpaired Student's t test.

SUPPLEMENTAL TABLES

Day0\Day2			Day2\Day0		
Cluster	*DAVID Functional Annotations*	*Score*	*Cluster*	*DAVID Functional Annotations*	*Score*
1	Cell cycle, M phase of mitotic cell cycle, mitosis, cell division	36.62	1	Extracellular region part, extracellular space	13.26
2	Condensed chromosome, centromeric region, kinetochore	18.60	2	Proteinaceous extracellular matrix, extracellular matrix	10.55
3	Chromosomal part, intracellular non-membrane-bounded organelle, cytoskeleton	15.34	3	Extracellular region, transmembrane region, intrinsi/integral to membrane, signal peptide	5.59
4	DNA replication, DNA metabolic process	9.50	4	Cell adhesion, biological adhesion	4.50
5	Spindle, microtubule. intracellular non-membrane-bounded organelle	8.51	5	Defense response, response to wounding, inflammatory response	3.91
6	DNA damage/repair, response to DNA damage cellular response to stress	8.06	6	Response to endogenous stimulus, to peptide hormone stimulus, to hormone stimulus	3.25
7	Microtubule-based process, spindle organization, cytoskeleton organization,	7.79	7	Regulation of cell adhesion, positive regulation of cell-substrate adhesion	3.13
8	Microtubule-based process/movement, Kinesin-motor region, microtubule	6.26	8	GTPase activity, Guanylate-binding protein	2.91
9	Cell cycle, ocyte meiosis, Progesterone-mediated oocyte maturation	5.83	9	Regulation of cytokine production, positive regulation of multicellular organismal process	2.80
10	Meiosis, M phase of meiotic cell cycle	5.77	10	Netrin domain, Netrin module, non-TIMP type	2.77
Cluster	*GSEA Hallmark Gene Set*	*p-val*	*Cluster*	*GSEA Hallmark Gene Set*	*p-val*
1	Genes involved in the G2/M checkpoint, as in progression through the cell division cycle.	1.8E-63	1	Genes up-regulated in response to IFNG [GeneID=3458].	7.1E-58
2	Genes encoding cell cycle related targets of E2F transcription factors.	1.4E-58	2	Genes regulated by NF-kB in response to TNF [GeneID=7124].	5.5E-39
3	Genes important for mitotic spindle assembly.	1.8E-30	3	Genes up-regulated in response to alpha interferon proteins.	1.3E-35
4	Genes encoding proteins involved in glycolysis and gluconeogenesis.	7.5E-07	4	Genes defining epithelial-mesenchymal transition, as in wound healing, fibrosis and metastasis.	1.1E-22
5	Genes defining late response to estrogen.	5.0E-06	5	Genes up-regulated by KRAS activation.	9.5E-21
6	Genes up-regulated during production of male gametes (sperm), as in spermatogenesis.	7.8E-06	6	Genes defining inflammatory response.	8.5E-20
7	Genes defining epithelial-mesenchymal transition, as in wound healing, fibrosis and metastasis.	3.0E-05	7	Genes up-regulated by IL6 [GeneID=3569] via STAT3 [GeneID=6774], e.g., during acute phase response.	1.6E-16
8	Genes encoding components of blood coagulation system; also up-regulated in platelets.	6.7E-05	8	Genes up-regulated during adipocyte differentiation (adipogenesis).	1.4E-13
9	Genes encoding components of apical junction complex.	1.7E-04	9	Genes involved in development of skeletal muscle (myogenesis).	1.4E-13
10	Genes defining inflammatory response.	1.7E-04	10	Genes down-regulated in response to ultraviolet (UV) radiation.	1.6E-13

Table S1: ***Distinctiveness in Maf1 biology prior to differentiation (Day 0) and 2 days after differentiation induction (day 2). Related to Fig. 7.***

Top ten DAVID enrichment clusters and top enriched GSEA Hallmark gene sets for presumtive Maf1 target genes uniquely expressed at Day 0 and Day 2, respectively. Day0\Day2 = {genes in Day0 but not in Day2}, Day2\Day0 = {genes in Day2 but not in Day0}. Only genes with p-val ≤ 0.01 and ≥ 2x Fc normalized RNAseq expression values were used for the analyses. Score: DAVID enrichment score for the annotation cluster.

Cluster	*DAVID Functional Annotations*	*Score*	*Genes*
1	Fat cell differentiation, brown fat cell differentiation, glucose homeostasis	6.54	ADIPOQ, ADRB2, BNIP3, CEBPA, EGR2, FABP4, LPIN1, MRAP, PEX11A, RETN, RGS2, SCD1, SH2B2, SLC2A4
2	Lipid metabolism, phospholipid/neutral lipid/triglyceride/ acylglycerol metabolic/catabolic/biosynthetic processes	3.90	ABHD5, ACSBG1, ACSL1, ADIPOQ, ADIPOR2, AGPAT9, DGAT1, DGAT2, FABP5, FLT1, GPD1, HSD11B1, LIPE, MGST3, PANK3, PIM3, PLIN1, PNPLA2, PNPLA3, SCD1
3	Response to insulin/to peptide hormone/ to endogenous stimulus	3.56	ACSBG1, ADIPOQ, ADIPOR2, EGR2, FABP4, FOXO1, LPIN1, RETN, SH2B2
4	Cell/membrane fraction, microsome, vesicular fraction	2.34	ACSBG1, ACSL1, ADRB2, DGAT1, DGAT2, GPD1, MGST3, PCDHGB8, RHOB, SLC2A4
5	Glucose/hexose/monosaccharide/carbohydrate transport	1.94	FABP5, KLF15, SLC2A4
6	Glucose/hexose/monosaccharide metabolic processes	1.39	ADIPOQ, ALDOA, FABP5, GPD1
7	Palmitate, S-palmitoyl cysteine, lipoprotein, positive regulation of developmental process	1.13	ADRB2, ALPL, CD36, RHOB, RHOV, SLC2A4, TSPAN12
8	Tube development, regulation of cell proliferation	1.01	ADRB2, AGT, CEBPA, FABP4, FLT1, FOXO1, HSD11B1, NOG
9	Identical protein binding, protein homodimerization activity	0.98	ADIPOR2, ADRB2, CEBPA, FLT1, GPD1
10	Positive regulation of protein kinase cascade/ Positive regulation of signal transduction	0.95	AGT, ADIPOQ, ADRB2
Cluster	*KEGG Pathways*	*p-val*	*Genes*
1	mmu03320:PPAR signaling pathway	5.6E-06	SCD1, ACSL1, CD36, PLIN1, FABP4, ADIPOQ, FABP5
2	mmu04920:Adipocytokine signaling pathway	4.0E-05	ACSL1, CD36, SLC2A4, ADIPOR2, ADIPOQ, PPARGC1A
3	mmu00830:Retinol metabolism	0.01	RDH12, BCMO1, DGAT1, DGAT2
4	mmu04910:Insulin signaling pathway	0.01	SLC2A4, FOXO1, SH2B2, PPARGC1A, LIPE
5	mmu00561:Glycerolipid metabolism	0.03	DGAT1, DGAT2, PNPLA3
Cluster	*GSEA Hallmark Gene Set*	*p-val*	*Genes*
1	Genes up-regulated during adipocyte differentiation (adipogenesis).	1.4E-17	ADIPOQ, ADIPOR2, ALDOA, CD36, CMBL, DGAT1, FABP4, LIPE, MGST3, MRAP, ORM1, PIM3, RETN
2	Genes encoding proteins involved in metabolism of fatty acids.	8.1E-09	ACSL1, ADIPOR2, ALDOA, CA2, CD36, G0S2, GPD1
3	Genes involved in metabolism of bile acids and salts.	3.6E-05	ACSL1, BCAR3, LIPE, PEX11A
4	Genes up-regulated in response to ultraviolet (UV) radiation.	1.4E-04	ALDOA, CA2, DGAT1, RHOB
5	Genes up-regulated by KRAS activation.	3.3E-04	CA2, G0S2, HSD11B1, RETN
6	Genes involved in myogenesis.	3.3E-04	ACSL1, BHLHE40, CD36, LPIN1
7	Genes regulated by NF-kB in response to TNF.	3.3E-04	BHLHE40, EGR2, G0S2, RHOB
8	Genes encoding proteins over-represented on the apical surface of epithelial cells	2.4E-03	ADIPOR2, SLC2A4
9	Genes up-regulated in response to TGFB1.	3.6E-03	BCAR3, NOG
10	Genes defining early response to estrogen.	4.4E-03	BHLHE40, ENDOD1, PEX11A

Table S2: ***Alteration of Maf1 expression and RNA pol III-dependent transcription regulates adipogenesis. Related to Fig. 7.***

Top enrichments for DAVID functional annotation clusters, KEGG pathways and GSEA Hallmark gene sets for presumtive Maf1 target genes at Day 2 that were concurrently up-regulated by Brf1 knockdown and ML-60218 treatment. Only genes with p-val $\leq$ 0.01 and $\geq$ 1.7x Fc normalized RNAseq expression values were used for the analyses. Score: DAVID enrichment score for the annotation cluster.

qPCR primers for mouse cell lines		
Targets	**forward**	**Reverse**
Maf1	GACTATGACTTCAGCACAGCC	CTGGGTTATAGCTGTAGATGTCAC
pre-tRNA$_i^{Met}$	CTGGGCCCATAACCCAGAG	TGGTAGCAGAGGATGGTTTC
pre-tRNA^{Leu}	GTCAGGATGGCCGAGTGGTCTAAG	CCACGCCTCCATACGGAGAACCAGAAGACCC
U6 RNA	GGAATCTAGAACATATACTAAAATTGGAAC	GGAACTCGAGTTTGCGTGTCATCCTTGCGC
GATA4	GATGGGACGGGACACTACCTG	TGGCAGTTGGCACAGGAGA
GATA6	GACGGCACCGGTCATTACC	ACAGTTGGCACAGGACAGTCC
T	GCTCTAAGGAACCACCGGTCATC	ATGGGACTGCAGCATGGACAG
Mesp1	GTTCCTGTACGCAGAAACAGCATC	TCAGACAGGGTGACAATCATCCG
Nestin	GCTTAGAGGTGCAGCAGCT	CTGTAGACCCTGCTTCTCCTGCT
Sox1	AGGCAGCTGGGTCTCAGAA	GACTCTGTGGTGGTGAGGTC
Oct4	GTGGAGGAAGCCGACAACAATGA	CAAGCTGATTGGCGATGTGAG
SOX2	CAGGAGAACCCCAAGATGCACAA	AATCCGGGTGCTCCTTCATGTG
Nanog	TGGTCCCCACAGTTTGCCTAGTTC	CAGGTCTTCAGAGGAAGGGCGA
PPARγ	ATCATCTACACGATGCTGGCCT	TGAGGAACTCCCTGGTCATGAATC
C/EBPα	GAACAGCAACGAGTACCGGGTA	CCATGGCCTTGACCAAGGAG
FABP4	TGGGAACCTGGAAGCTTGTCT	TCGAATTCCACGCCCAGTTTGA
Brf1	GGAAAGGAATCAAGAGCACAGACCC	GTCCTCGGGTAAGATGCTTGCTT
β-actin	CGACAACGGCTCCGGCATG	CTGGGGTGTTGAAGGTCTCAAACATG
PPia1	CGAGCTGTTTGCAGACAAAGTTCC	CCCTGGCACATGAATCCTGG
GAPDH	GATGGGTGTGAACCACGAGAA	GGGCCATCCACAGTCTTCTG
H19	AGCAGTGATCGGTGTCTCGAAGA	CCATCACACCGGACCATGTCAT
Wnt6	GCAAGACTGGGGTTCGAGAA	GCCTGACAACCACACTGTAGGAG
qPCR primers for human ES cells		
Targets	forward	Reverse
Maf1	GACTATGACTTCAGCACAGCC	CTGGGTTATAGCTGTAGATGTCAC
pre-tRNA$_i^{Met}$	CTGGGCCCATAACCCAGAG	TGGTAGCAGAGGATGGTTTC
pre-tRNA^{Leu}	GTCAGGATGGCCGAGTGGTCTAAG	CCACGCCTCCATACGGAGAACCAGAAGACCC
U6 RNA	GGAATCTAGAACATATACTAAAATTGGAAC	GGAACTCGAGTTTGCGTGTCATCCTTGCGC
Oct4	GACAGGGGGAGGGGAGGAGCTAGG	CTTCCCTCCAACCAGTTGCCCCAAAC
GAPDH	GATGGGTGTGAACCACGAGAA	GGGCCATCCACAGTCTTCTG

Table S3: ***qPCR primers list. Related to experimental procedures.***
qPCR primers for analyzing the expression of target genes in human and mouse cell lines.

SUPPLEMENTAL EXPERIMENTAL PROCEDURES

Cell culture

46C mESCs were cultured on 0.1% gelatin coated plates. GMEM medium was used to maintain the mESCs (Sigma-Aldrich, G5154) and it was supplemented with 15% ESC-qualified FBS (Life technologies), 0.1 mM MEM non-essential amino acids (NEAA), 2 mM GlutaMax, 1 mM Sodium Pyruvate, 0.1 mM β-mercaptoethanol, 1% penicillin/streptomycin, 100 units/ml LIF. H9 hESCs were maintained on matrigel-coated plates with MEF-conditioned medium consisting of DMEM/F12 supplemented with 20% knockout serum replacement (Life technologies), 0.1 mM MEM NEAA, 0.1 mM β-mercaptoethanol, 1% penicillin/streptomycin, and 4 ng/ml recombinant human FGF2 (Invitrogen). 3T3L1 mouse preadipocyte, MEF, and HEK293T cells were maintained in DMEM-HG supplemented with 10% FBS, 2 mM GlutaMax, and 1% penicillin /streptomycin. The SVF cells were cultured in DMEM-F12 supplemented with 10% FBS, 2 mM GlutaMax, and 1% penicillin /streptomycin. All cells were cultured in incubators with 5% CO_2 at 37ºC.

Isolation of mouse stromal vascular fraction (SVF) cells

The SVF cells were isolated from inguinal white adipose tissue. Male C57 BL/6J mice (6-8 weeks old) were euthanized in isoflurane chamber. The inguinal white adipose tissue from a mouse was washed by PBS and dried quickly on napkins. The tissue was then minced into small pieces and digested in 3 ml Type I Collagenase (3 mg/ml, Gibco) in SVF cell culture medium for 1 hour at 37ºC. After digestion, the mixture was centrifuged at 750 x g for 10 minutes, and the supernatant was carefully removed. The pellet was resuspended in 1 ml SVF culture medium and passed through 40 μm cell strainer. The filtered cell mixture was then centrifuged at 750 x g for 10 minutes, and the supernatant was carefully removed. The pellet was resuspended in SVF culture medium and plated on 6-well plates (The SVF cells from one mouse can be plated into three 6-well plates). 16-20 hours after plating the cells, media was changed.

Production of lentiviral constructs

Non-silencing empty vector control, pLKO.1-mouse Maf1 shRNA (clone IDs: TRCN0000125776 and TRCN0000125778), and pLKO.1-mouse Brf1 shRNA (clone ID: TRCN0000119897) were purchased from Sigma-Aldrich. The inducible pFTREW-Maf1-HA expression construct and FUIPW-rtTA (lentiviral tetracycline transactivator) was previously described (Palian et al., 2014).

Lentiviral particles were produced as previously described. Virus-containing media was collected, and sterile filtered through a 0.45 μm filter. Viruses were then concentrated by Lenti-X concentrator (Clontech), pelleted at 1,500 x g for 45 minutes at 4ºC, and resuspended in DPBS. Cell lines were transduced with the concentrated virus for 16 to 24 hours. Two days after transduction, the infected cells were selected with puromycin.

In vitro differentiation of ESCs

For mouse embryoid body (EB) formation, mESCs were dissociated with Accutase (Life technologies). 150,000 cells/ml mESCs were cultured in mESC medium without LIF on 6-well Ultra-Low attachment plates (Corning). For human EBs formation, 100,000 cells/ml hESCs were cultured in DMEM/F12 supplemented with 10% FBS on 6-well Ultra-Low attachment plates. For both mouse and human EBs, media was changed every other day. EBs were collected at the indicated time points described in the figures.

Differentiation of mESCs, 3T3-L1, MEF, and SVF cells into adipocytes

For the differentiation of mESCs into adipocytes, mESCs were first dissociated to form EBs. Two days after mEBs formation, mEBs were collected, and 10 to 20 mEBs were transferred to a well of gelatin-coated 6-well plates with mESC medium without LIF. On day 3, media containing 1 μM retinoic acid (RA) and 12.5 μg/mL ascorbic acid (AsA) was added, and changed every day until day 7. After day 7, media containing 0.5 μg/mL Insulin, 3nM triiodothyronine (T3), and 12.5 μg/mL AsA was added, and changed daily up to day 11. On day 12, the attached EBs were dissociated by Accutase (Life technologies), and 100,000 cells per well of a 6-well plate were re-plated in differentiation medium with the same hormone cocktail as day 7 to 11. The media was changed daily until day 15. After day 15, the medium was changed every other day and included 0.5 mM 3-isobutyl-1-methyl xanthine (IBMX), 0.1 μM Dexamethasone (Dex), 20 μg/mL Insulin, 0.06 mM indomethacin, and 25 μg/mL AsA until day 21. From day 21 to the end of the differentiation (approximately day 27), the media was changed daily and included 20 μg/mL Insulin, 25 μg/mL AsA, 3 nM and T3.

To differentiate the 3T3-L1 and MEF cells into adipocytes, cells were first grown to confluency. The 2-day post-

confluent cells were induced to differentiate with the differentiation cocktail which contained 10 µg/mL Insulin, 2 µM Dex, 0.5 mM IBMX and 25 µg/mL AsA. The duration of differentiation cocktail treatment varied in different experiments, and was between 2 to 6 days (Figure S1). During the treatment of the differentiation cocktail, the media was changed every 3 days. After the differentiation cocktail was no longer used in the media, the media was changed every other day and contained 10 µg/mL Insulin, and 25 µg/mL AsA until the differentiated cells were collected and analyzed.

To differentiate the SVF cells into adipocytes, cells were first grown to confluency, and were induced to differentiate with the differentiation cocktail which contained 10 µg/mL Insulin, 2 µM Dex, and 0.5 mM IBMX for two days (Figure S1). After incubation with the differentiation cocktail for two days, the media was changed every other day contained 10 µg/mL Insulin until the differentiated cells were collected and analyzed.

To prepare the media for the differentiation of 3T3-L1 cells in Biotin-free condition, the media containing 10% dialyzed FBS (Gibco), 2 mM GlutaMax, and 1% penicillin/streptomycin was incubated with avidin agarose resin (Pierce, 0.25 ml resin for 50 ml medium) at room temperature for 1 hour. The resin was removed by centrifugation at 500 x g, and used for the differentiation of 3T3-L1 cells following the same protocol as above.

RNA Pol III inhibitor treatment

The RNA Pol III chemical inhibitor, ML-60218 (Millipore), was dissolved in DMSO at a final concentration of 25 mM. The inhibitor was added to the cells at 20µM or 40 µM one day before the differentiation cocktail was added, and removed 2 days later. The control cells were treated with an equal volume of DMSO.

RNA isolation and Quantitative Real-Time PCR

Total RNA was isolated from cells using the Zymo Directzol RNA Kit. The RNAs were then reverse-transcribed into cDNA with the Superscript III first strand synthesis Kit (Invitrogen). Real-time quantitative PCR was performed on the Lightcycler 480 (Roche) with SYBR fast qPCR kit (KAPA Biosystems). Relative amounts of transcripts were quantified by comparative threshold cycle method (ΔΔCt) with GAPDH or β-actin as the endogenous reference control. The primers for targets are listed in Table S3. For statistical analysis, unpaired, two-tailed, student's *t*-test was used for all comparisons. All results are from three biological and two technical replicates.

Immunoblot analysis and antibodies

Cells were washed with DPBS twice, then scrapped and pelleted at 400g for 5 minutes. After removing the supernatant, the cells were lysed in triple lysis buffer, (50 mM Tris-Cl pH 8.0, 150 mM sodium chloride, 0.02% w/v sodium azide, 1% w/v SDS, 1 % v/v NP-40, 0.5% w/v sodium deoxycholate, containing protease inhibitor cocktail set III (EMD Millipore)) for 20 minutes on ice, and sonicated for 15 seconds. After sonication, the cells were centrifuged for 20 minutes at 10,000g, and the supernatant was collected. The protein concentration was determined by using the Biorad Protein *Dc* assay. Cell lysates were subjected to immunoblot analysis and transferred onto a nitrocellulose membrane (GE-Healthcare). Membranes were probed using the following antibodies: Maf1 (Abgent), PPARγ, C/EBPα, FABP4, and Perilipin (Cell Signaling), HA (Roche), T (Santa Cruz), Brf1 (Bethyl), β-actin (Sigma Aldrich), α-tubulin (Invitrogen). Protein bands were quantified using Image Lab software (Bio-Rad).

Immunohistochemistry

For Alkaline Phosphatase (AP) staining, 46C mESCs were cultured on 0.1% gelatin coated plates with culture conditions as described above for maintaining the mESCs. After two days, the cells were washed with DPBS twice, and fixed with 4% paraformaldehyde for 10 minutes. The fixed cells were washed with DPBS twice and stained using the Vectastain ABC-AP kit (Vector Laboratories). After staining, the cells were washed three times with DPBS.

For Oil-red O staining, the differentiated adipocytes from mESCs, 3T3-L1, and MEF cells were washed twice with DPBS, and fixed with 4% paraformaldehyde for 10 minutes. The fixed cells were washed with DPBS twice and stained with 0.3% Oil-red O solution (Sigma-Aldrich) for 15 minutes. After staining, the cells were washed three times with DPBS. The pictures were taken using the EVOS XL imaging system at the Human Stem Cell core at Baylor College of Medicine. For quantification, the dye was extracted by 100% isopropanol, and the intensity of Oil-red O extracts was quantified by measuring absorbance at 490 nm.

Immunostaining

Control and Maf1 knockdown mESCs were plated on 12-well plates. 48 hours later, the cells were fixed with 4% paraformaldehyde for 10 minutes, and blocked using 10% normal goat serum for 1 hour at room temperature. After blocking, the cells were incubated with primary SSEA1 antibody (University of Iowa, Developmental Studies Hybridoma Bank) at a dilution of 1:500, overnight at 4^{o} The next day, the cells were incubated with Alexa Fluor 488 (Molecular Probes) secondary antibody at a dilution of 1:250 for 1 hour at room temperature. After washing with PBS, the cells were incubated with DAPI solution (Sigma-Aldrich) at 0.05 μg/ml for 10 minutes at room temperature. The images were captured using a Zeiss Axiovert 200 microscope with a DVC-1310C digital camera (DVC).

Transfection

SVF cells were plated on 6-well plates, and transfected with 100 nM mismatched RNA (mmRNA) and Brf1 siRNAs using Lipofectamine RNAiMax transfection reagent (Invitrogen) according to the manufacturer's instructions. The cells were incubated with the transfection mixture for 48 hours. siRNAs against mouse Brf1 (SASI_Mm01_00136903 (siBrf1-1), SASI_Mm02_00333493(siBrf1-2)) were purchased from Sigma-Aldrich. The transfected SVF cells were then differentiated into adipocytes.

293T cells were plated on 24-well plate, and co-transfected with PPREx3-TK-Luc reporter (0.2 μg) (Addgene) which contains three copies of the PPARγ-respose element (PPRE) upstream of the luciferase gene, and a plasmid expressing Renilla luciferase (0.05 μg), and either PPARγ from pCDH-PPARγ (0.1 μg) (acquired from Sean Hartiq at BCM which is kindly provided by Fred Schaufele at UCSF), and Maf1 from pCDNA3(-)-Maf1-HA (0.1 μg) (previously described (Johnson et al., 2007)) using Fugene 6 transfection reagent (Promega). The transfected 293T cells were then used for luciferase reporter assay.

Luciferase reporter assay

24 hours after transfection of the 293T cells as described above, cells were treated with and without rosiglitazone (1 μM) for another 24 hours. Cells were harvested, and luciferase activity was measured using the Dual-Luciferase Reporter Assay System (Promega) according to the manufacturer's instructions with a microplate reader (BioTek Synergy2). The results were normalized to Renilla luciferase activity.

RNAseq and Data Analysis

Purified RNA was processed for RNA-Seq analysis and sent to EA|Q2 Solutions for library preparation and sequencing. Samples were prepared and sequenced according to a standard TS Stranded mRNA sequencing protocol using HiSeq-Sequencing-2x50bp-PE sequencing on an Illumina sequencing platform. RNA samples were converted into cDNA libraries using the Illumina TruSeq Stranded mRNA sample preparation kit (Illumina). After sequencing, initial analysis with a focus on qualtity control and gene quantification was performed using the RNAv9 pipeline developed by EA|Q2 Solutions. Across all samples, the median number of actual reads was 37 million with 36.1 million on-target reads. Mouse mm10 reference includes 31,252 genes of which our samples had a median of 13,814 (44%) genes detected. Clipping percentage was low with less than 1.2% of reads removed due to low quality, and the rank correlation to External RNA Controls Consortium RNA spike-ins (ERCCs) was determined ~94% % and with a slope of a best least-squares line 92% (0% of the reads aligned to the spike-in control sequences). The adjusted read depths ranged from 34.9 to 39 million with a median of 37 million, indicating high sequencing depth, which allows for consistent quantification of the expression levels with relatively high precision. To provide a robust estimate of fold change, the experimental and control values in the ratio are computed using medians. *p*-values were determined using a standard t-test assuming equal variance between groups. A relational database management system (FileMaker Pro 15) was used to filter genes for significance and fold change (all data shown in this manuscript are p-val $\leq$ 0.01 and $\geq$ 2x Fc normalized RNAseq expression values). Database for Annotation, Visualization, and Integrated Discovery Bioinformatics Resources (DAVID) v6.7 (http://david.abcc.ncifcrf.gov/), the KEGG (Kyoto Encyclopedia of Genes and Genomes) pathway database (http://www.genome.ad.jp/kegg/)) and GSEA (Gene Set Enrichment Analysis) on the Molecular Signatures Databases (MSigDB) collection (gsea@broadinstitute.org) analyses were used on filtered gene groups to identify enriched biological themes. The raw datasets and lists of differentially regulated transcripts were deposited to NCBI GEO (Accession number GSE113324.

SUPPLEMENTAL REFERENCES

Johnson, S.S., Zhang, C., Fromm, J., Willis, I.M., and Johnson, D.L. (2007). Mammalian Maf1 is a negative regulator of transcription by all three nuclear RNA polymerases. Molecular cell *26*, 367-379.

Palian, B.M., Rohira, A.D., Johnson, S.A.S., He, L., Zheng, N., Dubeau, L., Stiles, B.L., and Johnson, D.L. (2014). Maf1 is a novel target of PTEN and PI3K signaling that negatively regulates oncogenesis and lipid metabolism. PLoS Genetics *10*, e1004789.